Kisspeptin cell-type and fiber projection analysis suggests its potential role in central sensorial processing and behavioral state control

Running title: Kisspeptin cells molecular signature and projection mapping

Limei Zhang[1,6,7,8,c], Vito S. Hernández[1,6,7,c], Mario A. Zetter[1,7], Rafael Hernández-González[2], Oscar R. Hernández-Pérez[1], Ignacio Camacho-Arroyo[3], Lee E. Eiden[6,8], Robert P. Millar[1,4,5,8]

[1]Dept. Physiology and [2]Vivarium, School of Medicine, [3] Research Unit in Human Reproduction, National Institute of Perinatology-Faculty of Chemistry, Universidad Nacional Autónoma de México, México; Mexico City, Mexico
[4]Centre for Neuroendocrinology, University of Pretoria, and [5]Dept. of Integrative Biomedical Sciences, Institute of Infectious Disease and Molecular Medicine, University of Cape Town, South Africa;
[6]Section on Molecular Neuroscience, NIMH-IRP, NIH, Bethesda, MD, USA;
[7]These authors share first authorship
[8]These authors share the senior authorship
[c]Correspondence: either to limei@unam.mx or vitohdez@unam.mx

Abstract

Kisspeptin (Kp) is a neuropeptide well-established as the master regulator of the mammalian reproductive axis. However, information on Kp neuronal chemotype and distribution, especially in extra-hypothalamic brain regions, is incomplete, and has limited understanding of how Kp neurons function to affect behavior beyond direct effects on LH-RH release and activation of the hypothalamo-pituitary gonadal (HPG) axis. We therefore examined the chemotype (molecular signature) and fiber distribution of Kp neurons throughout the brain in mice and rat. Serial immunohistochemical sampling employing dual in situ hybridization with mRNA probes for kisspeptin and VGAT, VGLUT2, neurokinin, dynorphin, estrogen receptors, and androgen receptor was used for neuroanatomical analysis. Five distinct types of Kp-expressing cell populations distinguished by molecular signature were identified. One hundred sixteen brain regions were observed to contain Kp fibers and terminals, and eighty-one of these were extra-hypothalamic regions closely involved in central sensory processing and behavioral state control. This study provides an anatomical basis for further hypothesis generation and testing for the role of Kp in a wider scope of brain function than previously envisaged.

key words: Dual in situ hybridization (DISH), Esr1, Esr2, Ar, Slc32a1, Slc17a6, Tac2, Pdyn, behavior state system, pain sensitive pathway

Supported by: 1) grants: UNAM-PAPIIT-IG200121 and CONACYT-CF-243 (LZ), MH002386, NIMH, NIH, USA (LEE); 2) felloships: LZ and VSH were supported by sabbatical year fellowship to LEE's lab in NIMH/NIH, USA, from the PASPA program of the Dirección General de Personal Académico (DGAPA) of the Universidad Nacional Autónoma de México (UNAM); MAZ was supported by the POSDOC program of DGAPA-UNAM and RPM was supported by PREI program provided of the DGAPA-UNAM for a sabbatical research stay in LZ's lab in UNAM, Mexico.

1. Introduction

The kisspeptins (Kps), which include Kp-54, Kp-14, Kp-13, Kp-10 (Kotani, Detheux et al. 2001), are neuropeptides first identified as products of the anti-metastasis gene KiSS-1(Lee, Miele et al. 1996), now simply called *KiSS-1*. Kps and their receptor (GPR54 or Kiss1r) have emerged as key players in the regulation of reproduction (see (Clarke, Dhillo et al. 2015, Lehman, Coolen et al. 2018) for review). Furthermore, kisspeptins are located within extrahypothalamic circuits, notably in the amygdala, where emotion and cognition are integrated and functionally linked to reproduction and reproductive behaviors (Pineda, Plaisier et al. 2017, Lopez-Ojeda and Hurley 2022, Mills, Yang et al. 2022).

There had been comprehensive anatomical studies on kisspeptin neuronal populations and fiber distributions in the brain of diverse animal species in the literature of the first decade after the discovery, albeit hypothalamus and reproductive functions were the main focus of those studies (Mikkelsen and Simonneaux 2009, Lehman, Hileman et al. 2013, Liu and Herbison 2016, Lehman, Coolen et al. 2018).

In this study, we used an exploratory research approach strategy, performing a systematic chemoanatomical analysis, in order to extend our knowledge of kisspeptin's role in brain function beyond the regulation of Gn-RH neurons of the hypothalamus, and control of the HPG axis. We examined Kp neurons molecular signature and fiber distributions in the whole rodent brain using a pan-specific KP antibody which recognizes the Kp decapeptide epitope within Kp-54, 14, 13 and 10, and an improved immunohistochemistry procedure followed in our laboratories, together with the dual in situ hybridization (DISH) method, to examine the molecular signature of the five Kp expressing neuronal populations and its density-modification upon gonadectomy. Data from study provides an anatomical basis for further hypothesis generation and testing of the role of Kp in a wider scope of brain function. In particular, it draws attention to the remarkable presence of Kp projections in central sensory and behavioral state control structures. We believe our report will be an accelerant to reconsideration of the role of kisspeptin in social and reproductive behavior in humans which has not been adequately 'reverse-translated' into animal models due to lack of such fundamental chemoanatomical knowledge.

2. Material and methods

2.1. Animals

Wistar rats (N=12, male = 6, female = 6) and C57BL/6 mice (N=20, male = 10, female = 10) were obtained from the local animal vivarium and housed three per cage under controlled temperature and illumination (12h/12h) with water and food *ad-libitum*. Mice subjected to gonadectomy were singly housed for recovery for one week after surgery and then returned with their cage mates. All animal procedures were approved by the local research ethics supervision commission (license number CIEFM-079-2020). We analysed two brains sectioned in the parasagittal plane and two brains sectioned in the coronal plane for each sex and species. To evaluate the effect of gonadectomy on the expression of kisspeptin through the brain of male and female mice, we compared the immunoactivity of 4 control vs. 4 gonadectomised (one-year post-surgery) mice.

2.2. Gonadectomy

2.2.1 Mouse ovariectomy

A dorsal approach to remove the ovaries was used (Stout Steele and Bennett 2011). Briefly, animals were anaesthetised with ketamine 90mg/kg + xylazine 20mg/kg i.p. under anaesthesia animals were placed in ventral recumbency and a 3cm/side squared region centred over the third lumbar vertebra shaved. The shaved area was disinfected with Povidone and 70% alcohol, and a sterile fenestrate drape was placed over it. A single midline dorsal incision approx. 1 cm long was made in the skin at the level of the bottom of the rib cage. The incision was moved laterally to cut the right and left abdominal walls. After cutting the wall (obliques and transverse abdominal muscles),

blunt dissection through the body wall with mosquito haemostats was performed. Forceps were gently and carefully introduced to retrieve and exteriorise the corresponding ovary. The ovary, ovarian vessels, and ligament were ligated with 4-0 synthetic absorbable sutures and cut. The wall muscle layers incision was closed with a 4-0 synthetic, monofilament, absorbable suture. The skin incision was closed with a subcuticular suture.

2.2.2 Mouse orchiectomy

For the excision of the testicles, we followed a midline incision technique (Sophocleous and Idris 2019). Briefly, animals were anaesthetised with ketamine 75mg/kg + xylazine 16mg/Kg i.p. and placed on the operating table on their back. The central ventral side of the scrotum area was disinfected with Povidone and 70% alcohol. A single incision on the ventral side of the scrotum (1cm long) penetrating the skin was performed. Each cremaster muscle was cut, and each testis was exposed by gently pulling it through the incision using blunt forceps. Cauda of the epididymis, caput epididymis, vas deferens, and testicular blood vessels were exposed while holding the testicular sack with sterile tooth forceps. A single ligature 4-0 synthetic absorbable suture around the vas deferens and blood vessels was made, prior to excision and gentle removal of the testis. The remaining content was replaced in each one of the testicular sacks. The skin incision was closed with a subcuticular suture.

2.3 Immunohistochemistry

Animals were deeply anaesthetised with *i.p.* injected sodium pentobarbital (100mg/kg). They were perfused transaortically with 0.9% saline followed by a cold fixative containing 4% paraformaldehyde in 0.1 M sodium phosphate buffer (PB, pH 7.4) plus 15% v/v saturated picric acid for 15 min. Brain tissues were rinsed immediately after the 15 min fixation lapse until the PB yellowish colour was fully cleaned. Brains were then sectioned the same day, using a Leica VT 1000S vibratome at 70µm thickness in the coronal and parasagittal planes and the immunohistochemical (IHC) reaction was performed the same day of the perfusion-fixation. This procedure yielded a more comprehensive IHC labelling than longer fixation and delayed IHC as previously reported and discussed (Zhang and Hernandez 2013). One of every three sections was selected, and sections from animals that would be compared (*i.e.*, female control *vs.* female gonadectomy) were incubated in the same vial. To block the unspecific antibody binding, sections were incubated for one hour in a solution consisting of 20% normal donkey serum (NDS) diluted in tris-buffered saline (TBS, pH 7.4) plus 0.3% Triton-X (TBST). After the blocking step, sections were incubated for 48h at 4ºC in a polyclonal sheep anti-kisspeptin antibody (Dhillo, Chaudhri et al. 2005) (GQ2, kindly supplied by Mohammad Ghatei†, Imperial College, London, UK), diluted at a 1:2000 concentration in TBST + 1% NDS. This antibody recognises kisspeptins 54, 14,13, and 10 that conserve the C-terminal decapeptide essential for biological activity and shows virtually no cross-reactivity (<0.01%) with other related human RF-amide peptides (Dhillo, Chaudhri et al. 2005). After three wash steps, sections were incubated for 24 hours with the secondary donkey anti-sheep biotinylated antibody (Cat: 713-065-147, Jackson ImmunoResearch Inc, PA, USA) diluted at a concentration of 1:500 in TBST + 1% NDS. To detect the biotinylated antibody, VECTASTAIN Elite ABC HRP Kit (Cat: PK-6100, Vector Laboratories, Inc. CA, USA) was used, with H2O2 and 3,3'-Diaminobenzidine as substrates. Finally, sections were mounted on glass slides, dehydrated, dipped in xylene, and cover-slipped using Permount™ mounting medium.

2.4 Dual in situ hybridization (DISH) procedure

Detailed methods are described elsewhere (Zhang, Hernandez et al. 2018, Zhang, Hernandez et al. 2020, Zhang, Hernandez et al. 2021). Briefly, male and female mice were deeply anaesthetised with sodium pentobarbital (Sedalpharma, México, 100 mg/kg b.w., i.p.) and decapitated using a small animal guillotine (Kent Scientific Corp.). Brains were removed and rapidly frozen by immersing in 2-methyl butane (Cat. M32631, Sigma-Aldrich, Darmstadt, Germany) previously chilled in dry ice. The fresh-frozen brains were sectioned in sagittal 12 µm thick sections with a Leica CM-1520 cryostat and mounted on positively charged Superfrost Plus microscope slides (Cat. 22-037-246, Fisher Scientific, Pittsburgh, PA). The probes used to detect the mRNAs in this double in-situ hybridisation (DISH) were designed by Advanced Cell Diagnostics (https://acdbio.com/rnascope-25-hd-duplex-assay) for kisspeptin

(Mm-Kiss1, channel 1 probe) and channel 2 (C2) for VGAT (Mm-Slc32a1-C2); for VGLUT2 (Mm-Slc17a6-C2); for neurokinin (Mm-Tac2-C2); for dynorphin (Mm-Pdyn-C2) and, estrogen receptors alfa (*Esr1,* RNAscope® Probe-Rn-Esr1-C2. 317151-C2) and beta (*Esr2,* RNAscope® Probe-Rn-Esr2. 317161) and androgen receptor (*Ar,* RNAscope® Probe-Rn-Ar. 317141). All experimental steps were performed following the provider's protocol. Briefly, after sectioning, slides were fixed in chilled 4% paraformaldehyde (Cat. 30525-89-4, Sigma-Aldrich) prepared in phosphate-buffered saline (Cat. M32631, Sigma-Aldrich), dehydrated in ethanol, treated with hydrogen peroxide for 15 minutes, protease plus 30 minutes at room temperature, incubated for two hours in a mixture of channel 1 and channel 2 probes, incubated with the amplification-detection reagents following the provider's protocol, counterstained with haematoxylin and coverslipped.

2.5 Anatomical assessment of kisspeptin innervation density and comparison between control and gonadectomised animals

To assess the projection patterns of kisspeptin immunopositive fibers through the brain, and to compare in detail with the comprehensive rat neuroanatomical study of Brailoiu and colleagues (Brailoiu, Dun et al. 2005) carried out using a human metastatin 45-54 rabbit polyclonal antibody from Phoenix Pharmaceuticals (see Mikkelsen and Simonneaux, 2009), three researchers independently examined the slides under a light microscope, after identifying the regions based on the Paxinos Rat & Mouse brain atlases. Scores of "+" (sparse, main axons passing, without branching nor axon terminals); "++", mild, some branching; "+++", moderate, abundant branching and axon terminals; "++++", intense, extensive branching and intense axon terminals, with confluent fibers that it was difficult to see a separation between them, were reported. It is worth noting that we consider this *ambiguous* scoring method more applicable for this anatomical assessment. Due to factors beyond the scope of our study, the IHC reactions on different subjects perfused-fixed at different circadian time points, yielded minor yet different labelling strengths. Hence, setting a quantitative measurement method on samples where variations existed due to other reasons can mislead our conclusion. In contrast, this semi-quantitative method, based on independent observations from three researchers, scoring on the best labeled samples, may yield more-objective conclusions toward the higher possibility of Kp expression reflected to a living animal, because the Kp-fibers and cells can only be visualized when the peptide was present at a given location, at the moment of perfusion-fixation, of a given experiment.

3. Results and discussion

3.1 Molecular signatures of kisspeptin-expressing neuronal populations in the mouse and rat brains

We used a sensitive dual ISH (DISH) method to study the co-expression of the mRNA of kisspeptin (*Kiss1*) with the vesicular GABA transporter (*Slc32a1*), vesicular glutamate transporter 2 (*Slc17a6*), neurokinin (*Tac2*), dynorphin (*Pdyn*), estrogen receptors alfa (*Esr1*) and beta (*Esr2*) and androgen receptor (*Ar*), in both mouse and rat brains, male and female, at the single-cell level in the five regions where kisspeptin-expressing neurons were identified. The chemotypes were first determined in mouse brains and were confirmed in rat brains. These latter ones were generally observed with stronger expression, however, we cannot assert these stronger expressions were due to biological differences between species or due to reagent sensitivities.

3.1.1 Kisspeptin mRNA Kiss1 expressing neuronal population in the antero-ventral periventricular region (AVPV) and medial preoptic area (MPO) of the hypothalamus

The most rostral neuronal population was observed in the medial preoptic area (MPO) and the antero-ventral periventricular area (AVPV) of hypothalamus, close to the wall of the third ventricle (3v) and the anterior commissure (ac) (see Fig. 1A, from the Allen mouse brain, reference atlas for anatomical location in para-sagittal plane). A dual in-situ hybridization (DISH) method allowed us to evaluate the co-expression of two mRNAs at single cell level, as can be observed in Fig. 1. The density and strength of expression of *Kiss1* was observed stronger in the MPO then in the AVPV (Fig. 1B). We first examined the co-expression nature of these neurons with sex-steroid receptor mRNA expression and found that the AVPV group strongly co-expressed *Esr1* (mRNA encoding

the estrogen receptor alfa, double blue/red arrows indicate co-expression) while the MPO seemed weakly express the *Esr1* (Fig. 1, panels B, Ba, Bb and Bc). Due to technical limitations, we could not obtain the combination for *Kiss1* vs. *Esr2* and *Kiss1* vs *Ar*, however, we performed DISH in adjacent sections of 12 microns, the combination of *Esr2* vs *Esr1* and *Ar vs. Esr1*. We found the ERa expressing neurons strongly co-express androgen receptor (Fig. 1, Be) and weakly express the ER beta receptor mRNA (Fig. 1, Bd). This observation demonstrates that the kisspeptin neurons in the AVPV/MPO regions are sensitive to estrogen via receptor alfa and it is likely that they are also expressing the ERb receptor, as well as sensitive to androgen via androgen receptor.

This neuronal population co-express *Kiss1* and *Slc32a1* (mRNA for VGAT, Fig. 1, Ca and Ca') and lacks to co-express *Slc17a6* (mRNA for VGLUT2, Fig. 1, Cb and Cb'). Most of Kiss1 expressing neurons co-express *Pdyn* (mRNA for dynorphin, Fig. 1, Cd and Cd') but are negative for *Tac2* (mRNA for neurokinin, Fig. 1, panels Cc and Cc').

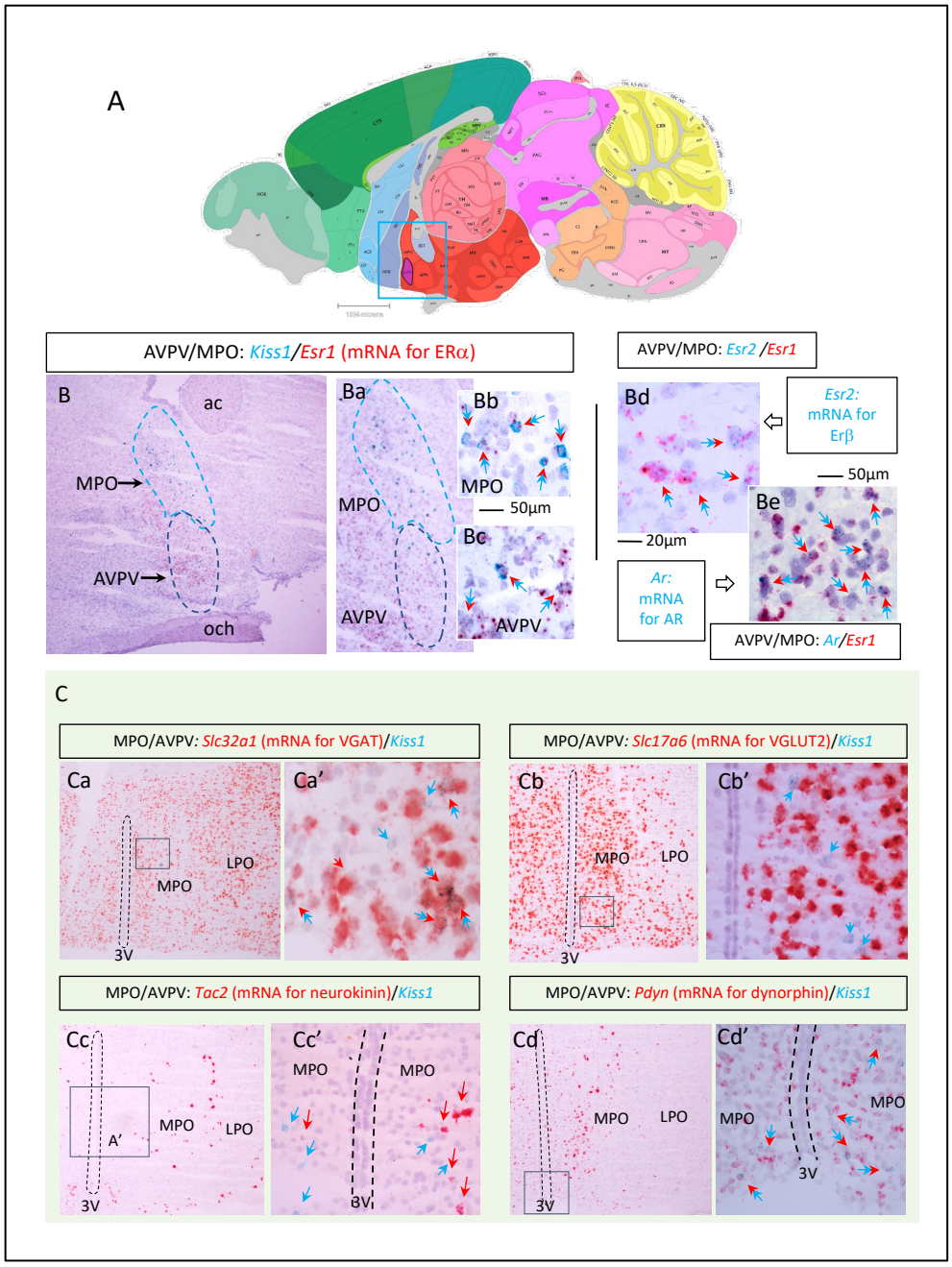

Fig. 1 Molecular signature of *Kiss1*-expressing cell populations in the hypothalamic medial preoptic area (MPO) and anteroventral periventricular (AVPV) region. (A) Parasagittal plane from the Allen brain reference atlas with squared region delimitating the MPO and AVPV regions. (B) Dual in-situ hybridization (DISH) experiments showed a higher density of Kiss1-expressing neurons (green) within the MPO than in the AVPV. The estrogen receptor alpha (Esr1) showed a stronger co-expression (double arrows) in the AVPV than in the MPO (Ba - Bc). Co-localization of *Esr1* with estrogen receptor beta (*Esr2,* panel Bd) and androgen receptor (*Ar,* panel Be) mRNA was observed. The Kiss1 neurons of this region co-express the mRNA for the vesicular GABA transporter (*Slc32a1*, panels Ca´s), and lacks the mRNA for the vesicular glutamate transporter 2 (*Slc17a6*, panels Cb´s). Also most *Kiss1*-expressing neurons co-express the mRNA for dynorphin (*Pdyn*) and are negative for neurokinin (Tac2, panels Cc´s).

3.1.2 Kisspeptin mRNA Kiss1 expressing neuronal populations in hypothalamic levels

At posterior hypothalamic levels, two populations of kisspeptin mRNA expresing neurons were observed. The most intensely labelled and numerous population was located in the arcuate nucleus (ARH, Fig. 2A and B), the other population was located dorsally in the dorsal hypothalamus (DH) and dorsomedial hypothalamic nucleus (DMH) with a more scattered distribution. Dual in-situ hybridisation showed that *Kiss1* neurons in ARH and DH/DMH were glutamatergic since they co-expressed the mRNAs for kisspeptin (*Kiss1*) and the vesicular glutamate transporter VGLUT2 (*Slc17a6*, panel Cs). In the ARH, the *Kiss1* expressing neurons strongly co-expressed *Esr1* (Fig. 2, Ba) and *Ar* (Fig. 2, Bc) but are not likely to co-express *Esr2* since most of the *Esr1* expressing cells was not observed to co-express *Esr2* (Fig. 2, Bb). Also, we confirmed that the *Kiss1* expressing neurons co-express the mRNA for neurokinin (*Tac2,* Fig. 2 Ea) and dynorphin (*Pdyn*, Fig. 2 Fa). The *Kiss1* positive neurons in these regions were not found to coexpress the mRNA for VGAT (Fig. 2, Ca). The *Kiss1* expressing neurons in DH co-express the *Slc17a6* (VGLUT2, Fig. 2 Db), and some of them expressed neurokinin (*Tac2,* Fig. 2 Eb), but not *Slc32a1* (VGAT, Cb) nor *Pdyn* (Fig. 2 Eb).

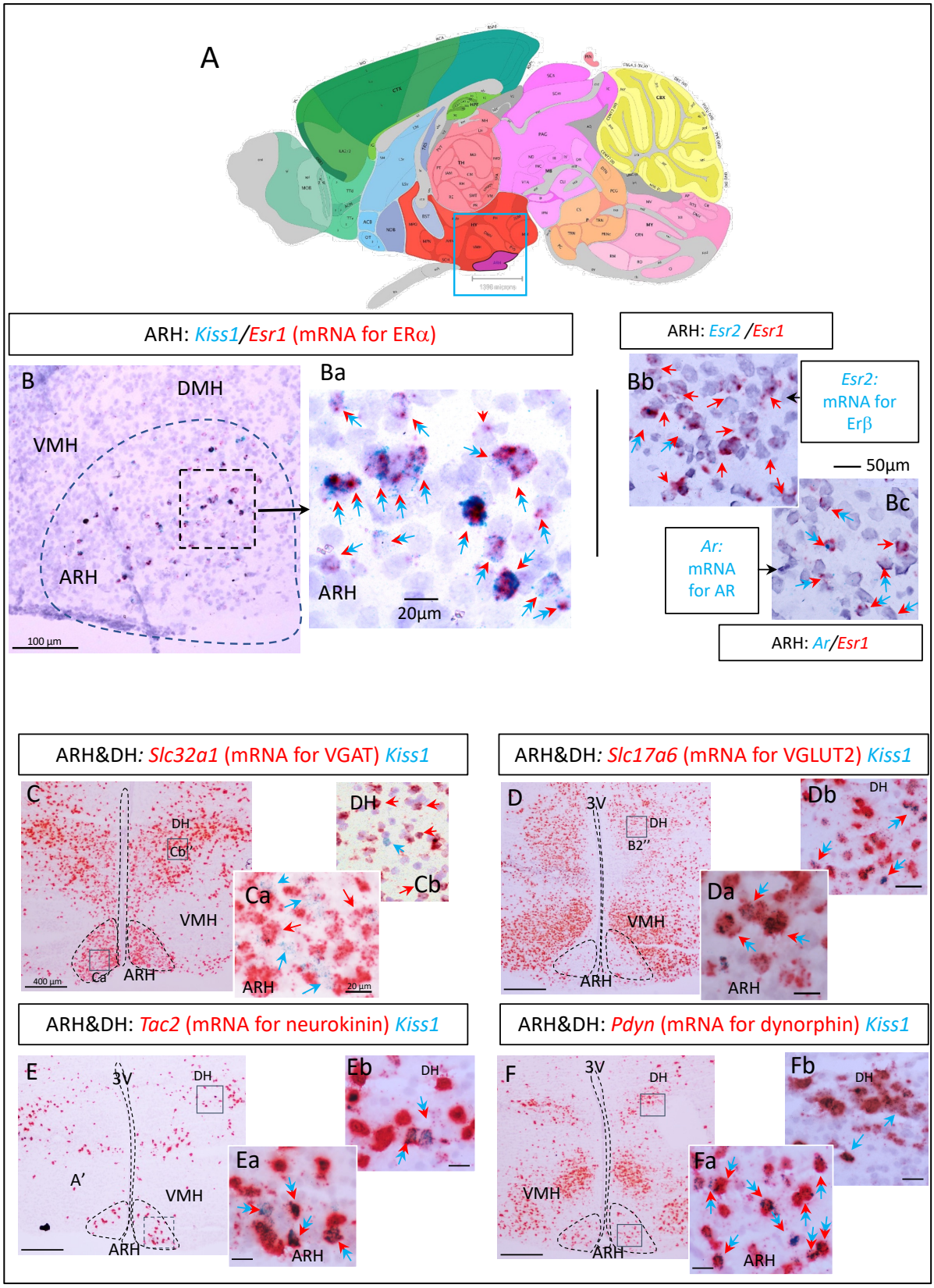
A
ARH: Kiss1/Esr1 (mRNA for ERα)
B
DMH
VMH
ARH
100 µm
Ba
ARH
20µm
ARH: Esr2 /Esr1
Bb
Esr2: mRNA for Erβ
50µm
Bc
Ar: mRNA for AR
ARH: Ar/Esr1
ARH&DH: Slc32a1 (mRNA for VGAT) Kiss1
C
DH
Cb''
VMH
Ca
ARH
400 µm
DH
Cb
Ca
ARH
20 µm
ARH&DH: Slc17a6 (mRNA for VGLUT2) Kiss1
D
3V
DH
B2''
VMH
ARH
Db
DH
Da
ARH
ARH&DH: Tac2 (mRNA for neurokinin) Kiss1
E
3V
DH
A'
VMH
ARH
Eb
DH
Ea
ARH
ARH&DH: Pdyn (mRNA for dynorphin) Kiss1
F
3V
DH
VMH
ARH
Fb
DH
Fa
ARH

Fig. 2 Molecular signature of *Kiss1*-expressing cell populations in hypothalamic arcuate nucleus and dorsal hypothalamus. (A) Parasagittal plane from the Allen brain reference atlas with squared region delimitating the arcuate nucleus (ARH) and dorsal hypothalamus (DH). The ARH *Kiss1* neuronal group co-expressed the mRNAs for estrogen receptor alpha (*Esr1,* panels B and Ba), vesicular glutamate transporter 2 (*Slc17a6*, panels D and Da), neurokinin (*Tac2*, panel E and Ea) and dynorphin (*Pdyn*, panel F and Fa), no colocalization with the vesicular GABA transporter (*Slc32a1*, panel C and Ca) was observed. Most Esr1-expressing neurons in the ARH co-expressed the androgen receptor (*Ar*, panel Bc). Few *Esr1*-expressing neurons co-expressed the estrogen receptor beta (*Esr2*, panel Bb). The DH neuronal group co-expressed VGLUT2 mRNA (*Slc17a6*, panel D and Db) and some *Kiss1* neurons co-expressed neurokinin (*Tac2*, panels E and Eb). No co-expression with the mRNAs for VGAT (*Slc32a1*, panels C and Cb), sex steroid receptors or dynorphin (*Pdyn*, panels F and Fb) was observed in the DH region.

3.1.3 Kisspeptin mRNA Kiss1 expressing neuronal populations in amygdala

The other population of neurons observed at this rostrocaudal level is a small population of GABAergic neurons in the medial postero-dorsal nucleus of the amygdala (MePD, Fig 3A and B). DISH experiment showed that the amygdalar kisspeptin (*Kiss1 mRNA*) neurons, co-expressed the vesicular GABA transporter VGAT (*Slc32a1 mRNA,* Fig. 3, B, C and C') but did not observed the co-expression of the mRNAs for VGLUT2 (*Slc17a6*, Fig. 3, D) nor neurokinin (*Tac2*, Fig. 3E) or dynorphin (*Pdyn*, Fig. 3 F). In term of expression of sex steroids receptors, these *Kiss1* expressing neurons co-expressed *Esr1* (ERα, Fig. 3E). Due the technical limitations we performe *Esr1* vs *Esr2* and *Esr1* vs *Ar* DISH experiments in subsequent sections that showed the likelihood that those Kisspeptinergic neurons could express ER beta and AR, though in weak expression levels. The chemoanatomical markers identifyed in this population of MePD cells are congruent with a recent study in which the authors used RNA-seq to identify over 13,800 transcripts co-expressed by MeA neurons that were *Kiss1/ Cck /Cartpt* positive (Hatcher, Costanza et al. 2023).

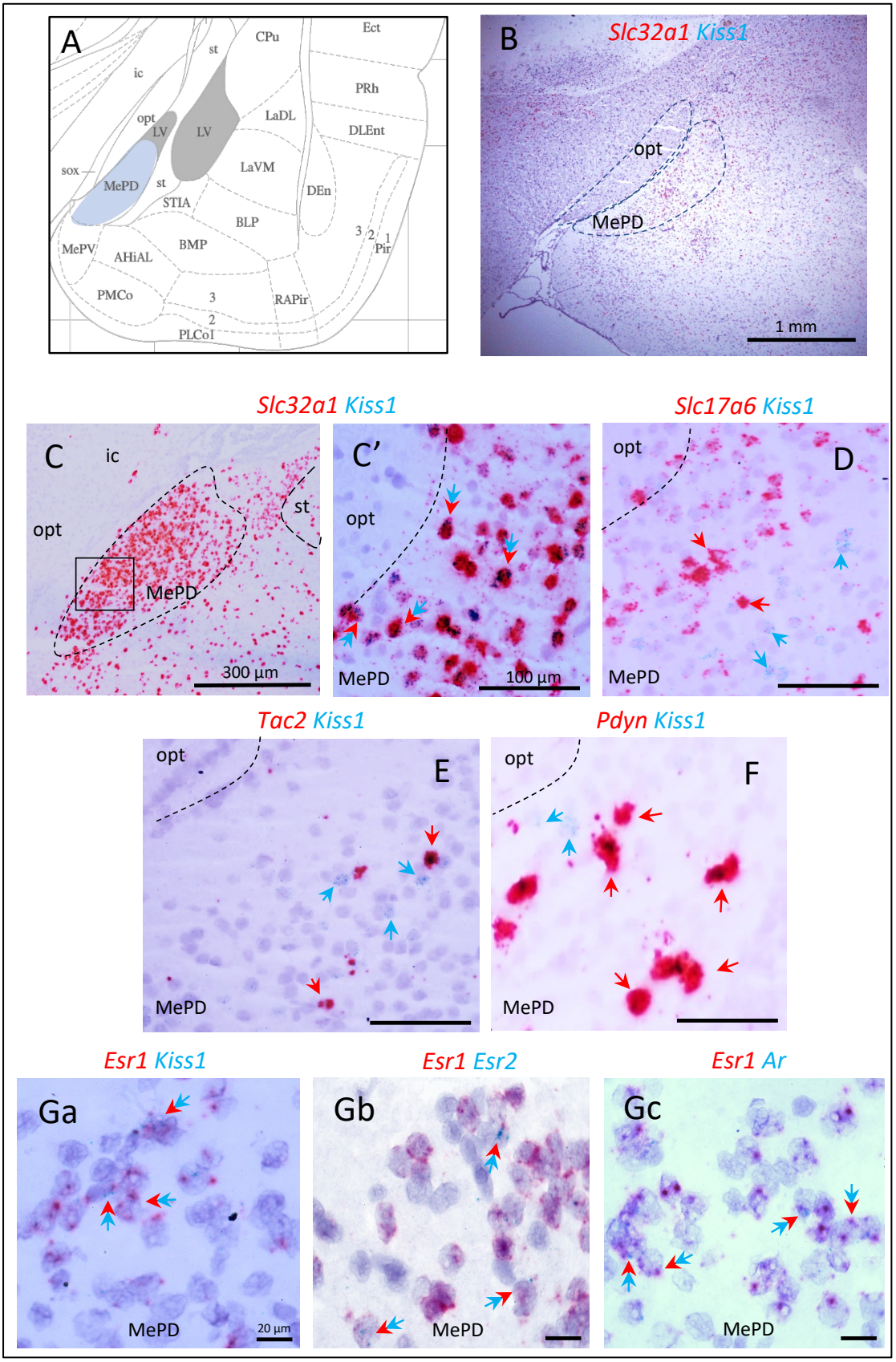
A
st
CPu
Ect
ic
PRh
opt
LV
LV
LaDL
DLEnt
sox
LaVM
MePD
st
DEn
STIA
BLP
3
2
1
Pir
MePV
BMP
AHiAL
PMCo
3
RAPir
2
PLCoI
B
Slc32a1 Kiss1
opt
MePD
1 mm
Slc32a1 Kiss1
C
ic
st
opt
MePD
300 µm
C'
opt
MePD
100 µm
Slc17a6 Kiss1
opt
D
MePD
Tac2 Kiss1
opt
E
MePD
Pdyn Kiss1
opt
F
MePD
Esr1 Kiss1
Ga
MePD
20 µm
Esr1 Esr2
Gb
MePD
Esr1 Ar
Gc
MePD

Fig. 3 Molecular signature of the *Kiss1*-expressing cell population in the posterodorsal division of the medial amygdala. (A) A segment of a coronal plane drawing of Paxinos mouse brain atlas, with the postero-dorsal division of the medial amygdala (MePD) colored in purple. (B) Low magnification photomicrograph of a dual in-situ hybridization (DISH) in the region of interest showing the expression of the mRNAs coding for the vesicular GABA transporter (*Slc32a1)* and Kisspeptin *(Kiss1)*. The *Kiss1* neurons showed co-expression with the mRNA for VGAT (*Slc32a1,* panels C and C′) but no overlap with mRNAs for VGLUT2 (*Slc17a6,* panel D), neurokinin (*Tac2*, panel E), nor dynorphin (*Pdyn,* panel F*).* The MePD *Kiss1* positive neurons co-expressed the mRNA coding for estrogen receptor alfa (*Esr1,* panel Ga). Most *Esr1* neurons co-expressed the mRNAs for estrogen receptor beta (*Esr2*, panel Gb) and for androgen receptor (*Ar*, panel Gc), suggesting that MePD kisspeptin neurons are estrogen- and androgen-sensitive via ER alfa, ER beta, and AR. Scale bars B: 1mm; C: 300µm; C′, D and E: 100µm; F: 50µm; Ga, Gb and Gc: 20µm.

3.1.4 Kisspeptin mRNA Kiss1 expressing neuronal populations in metencephalon

The metencephalic tractus solitarii (Sol) and area postrema (AP) host the most caudal population of the kisspeptinergic neurons. Figure 4 show the kisspeptin expressing in both peptide and mRNA levels. Figure 4A shows a charting where blue dots sybmolize the Kp neurons location within the dorsal part of Sol bordering with the AP; also dense networks of kisspeptin immunopositive axon terminals symbolised with red labellings were observed in this region. The photomicrographs of panels Aa-Ac, show the dense immunoreaction located in Sol, some kisspeptin immunopositive somas and a confocal picture of a kisspeptin immunopositive axon co-labelled with an antibody against VGAT. Dual *in-situ* hybridisation in panel Bs shows the GABAergic (*Slc32a1*) nature of this population of kisspeptin (*Kiss1*) neurons, that also co-express Esr1 and likely the Ar. These neurons did not express the mRNAs for VGLUT2 (*Slc17a6*), dynorphin (*Pdyn*) or neurokinin (*Tac2*) (not shown). Some projection targets of kisspeptin fibers in hindbrain regions (showed in panels C of the figure 4) were located in the external part of the lateral parabrachial nucleus (LPBe, Fig. 4, Ca), in the locus coeruleus (LC, Fig. 4, Cb) and in the sensitive nucleus of the trigeminal nerve specially in its gelatinous layer (Sp5 and Ge5, Fig. 4, Cc - Cd) also called substantia gelatinosa of Rolando (SGR)(Merighi 2018). The Kp axons were observed to make perisomatic contact with the neurons of the gelatinous layer sensitive nucleus of the trigeminal nerve (arrows in Fig. 4, Ce). The substantia gelatinosa of Rolando (SGR) is a grey matter structure of the dorsal spinal cord primarily involved in the transmission and modulation of pain, temperature, and touch (Sheikh and Dua 2023).

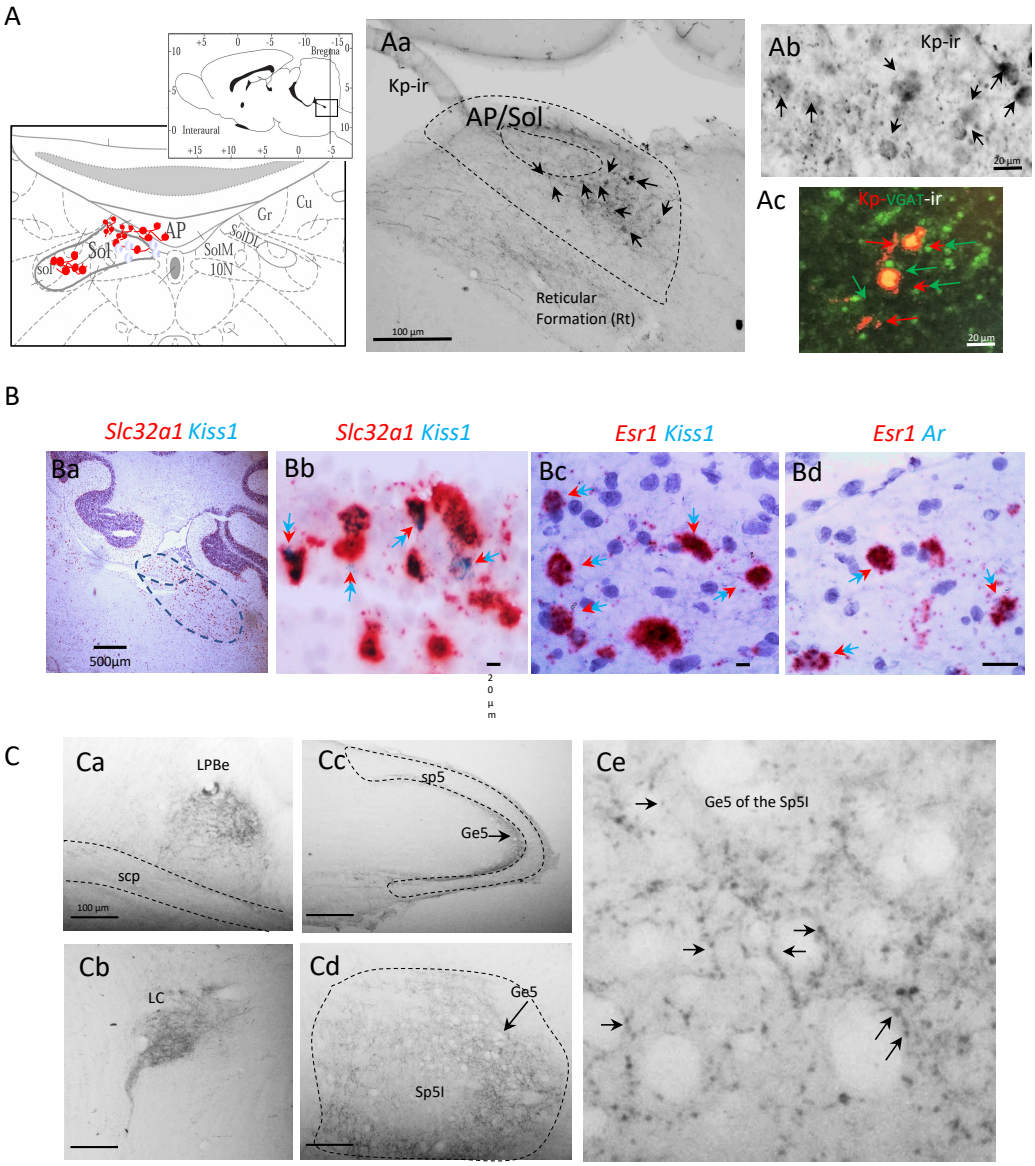

Fig. 4 Characterization of *Kiss1*-expressing populations in the metencephalon: (A) Atlas segment representing a coronal section, showing the metencephalic region where the most caudal population of *Kiss1* expressing neurons was found. Red dots and lines symbolize respectively the location of somas and fibers within the dorsal part of the nucleus of the solitary tract (Sol) and in the area postrema (AP). (Aa) Low amplification photomicrograph showing the dense kisspeptin immunoreaction (Kp-ir) in Sol/AP. (Ab) High amplification photomicrograph showing Kp-ir somas located within the Sol. (Ac) Confocal photomicrograph showing a Kisspeptin positive axon co-labelled with an antibody against the vesicular GABA transporter, VGAT. Panels B´s show the mRNA molecular signature of this population of neurons. (Ba and Bb) Low and high amplification photomicrograph of a dual in situ hybridization (DISH) reaction showing the co-expression of *Kiss1* (kisspeptin) and *Slc32a1* (VGAT) mRNAs in neurons located in Sol/AP regions. *Kiss1* expressing neurons were identified as expressing the estrogen receptor alpha mRNA (*Esr1*, panel Bc). Most of *Esr1* expressing neurons also co-expressed the androgen receptor mRNA (*Ar*, panel Bd). Dense networks of KP-fibers were observed in hindbrain regions, including the external part of parabrachial nucleus (LPBe, panel Ca), the *locus coeruleus* (LC, panel Cb) and the sensitive nucleus of the trigeminal nerve, especially on its gelatinous layer (Sp and Ge5, panels Cd and Ce). scp: superior cerebellar peduncle.

An overview of the five population of neurons in the mouse brain, characterized with regard to the coexpression of kisspeptin mRNA (*Kiss1*) with the mRNAs for VGAT (*Slc32a1*), VGLUT2 (*Slc17a6*), dynorphyn (*Pdyn*), neurokinin (*Tac2*) and estrogen receptor alpha (*Esr1*). As it was mentioned before, due to technical limitations we could not pair the *Kiss1* with the *Esr2* nor *Ar* (the available probes were ocupaying the same channels, *vide supra*). However, we made the DISH experiment paring *Esr1* with each of them in the immediate subsequent sections (12 microns of thickness). Neurons co-expressing the estrogen receptor alpha (*Esr1*) mRNA and the estrogen receptor beta (*Esr2*) or androgen receptor (*AR*) mRNA were reported (gray letters) in the table that represent certain likelihood of the co-expression or not of those two sex steroids receptors in a given region.

Table 1. Some molecular signature of the 5 populations of kiss1-expressing neurons in rodent

Co-expressing / *Kiss1* Expressing in	VGAT mRNA: Slc32a1 or Gad2 (GAD65)	VGLUT2 mRNA: *Slc17a6*	Neurokinin mRNA: *Tac2*	Dynorphin mRNA: *Pdyn*	Estrogen receptor α mRNA: *Esr1*	Estrogen receptor β mRNA: *Esr2 (vs. Esr1) in serial section*	Androgen receptor mRNA: *Ar (vs Esr1) in serial section*
MPO-AVPV	✓✓	✓	n.o.	✓	✓✓✓	✓	✓✓
Arc	n.o.	✓✓✓	✓✓✓	✓✓✓	✓✓✓ .	n.o.	✓✓
DH-TC	n.o.	✓	✓	n.o.	n.o.	n.o.	n.o.
MeApd	✓✓✓	✓	n.o.	n.o.	✓	✓	✓
Sol-AP	✓✓✓	n.o.	n.o.	n.o.	✓	✓	✓

Molecular signature of 5 population of neurons were characterized by the expression of the mRNAs (*italic lettering*) coding for VGAT: vesicular GABA transporter; GAD2: glutamate decarboxylase 2; VGLUT2: vesicular glutamate transporter 2; RP3V: rostro-periventricular area of the third ventricle; AVPe: anteroventral periventricular area; Arc: arcuate nucleus; DH-TC: dorsal hypothalamus - tuber cinereum area; MeApd-AHi: medial amygdala postero-dorsal - amygdalo-hippocampal area; Sol-AP: nucleus of the solitary tract - area postrema. n.o.: not observed. Rats showed stronger levels of Kiss1 mRNA than mice, however no differences in the co-expression patterns were observed thus a single table is presented.

3.2 Regional distribution of kisspeptin-expressing fibers and neurons in the mouse and rat brain

In this study, we performed Kp-IHC using the GQ2 antibody and a sensitive experimental method, with picric acid added to the conventional fixative, strict time frames for fixation, washing, and slicing, and initiation of the IHC reaction immediately after fixation, coupled with long incubation (2 days at 4ºC), to maximize reproducible visualization of Kp-positive fibers and neurons throughout the rodent brain. In table 2 (Tab. 2), we report 116 regions of the rodent brain in which we observed Kp-ir labelling with differential strengths. In general, the rat brain, in particular, in telencephalic regions *(vide infra*) exhibited stronger labelling than the mouse brain, however, no fundamental qualitative differences were detected between rodent species. Variabilities from experimental subjects and given immunoreactions were found. Sex differences regarding the distribution of cells or fibers were not consistent between experimental subjects, under the same experimental procedures. For instance, for a given region, some reactions were stronger than others and they were not consistently linked with sex of the experimental subject. Diverse factors which are out of our awareness may influence this observation. For instance, Kp expression can be up- or down- regulated in each organism by its own physiological regulation that cause the presence or absence of the peptide vesicles at a given location, at the moment of perfusion-fixation, i.e., a kisspeptinergic (referring the linkage to a neuron which can synthezise Kp) axon or dendrite can only be detected with Kp-IHC if the segment has the filling of the peptidergic vesicle at the moment of fixation. Based on this observation and rationale, we pooled the male and female data, for each rodent species (i.e. separation rat *vs.* mouse), to show the highest possible Kp expression in a given region as "ideal subjects", scoring the maximum density of the best sample in a given region. This analysis criterion would allow us to gain the knowledge toward the maximum expression potential of Kp in a living rodent.

In this table, we also made detailed comparison with a previous publication (Brailoiu, Dun et al. 2005) using an *anti-metastatin antibody*, that surprisingly it is one of the comprehensive reports in the literature that we found that had highest similarity to our data. All the regions reported in that study were confirmed in our experiments. However, numerous new regions were found containing Kp expressing fibers which were not included in their report. Figure 5 represents the Kp-ir fibers and cell bodies through the mediolateral extent of the rat brain (with comparable distribution in mouse brain).

Table 2. Distribution of kisspeptin immunoreactive (antibody GQ2) fiber distribution in mouse & rat brain with comparison of Brailoiu et al, JCN, 2005 (metastatin, MT)

Structure	Abbr.	irMT cells	irGQ2 mouse	irGQ2 rat	irMT fibers	irGQ2 mouse	irGQ2 rat
Telencephalon							
Cerebral cortex							
Cingular cortex	Cg	n.r.	-	-	n.r	+	+
Dorsal peduncular cortex	DP	n.r.	-	-	n.r	+	+
Dorsal tenia tecta	DTT	n.r.	-	-	n.r	+	+
Infralimbic cortex	IL	n.r.	-	-	n.r	+	+
Prelimbic cortex	PrL	n.r.	-	-	n.r	+	+
Ventral orbital cortex	VO	n.r.	-	-	n.r	+	+
Olfactory area							
Anterior olfactory nucleus	AON	n.r.	-	-	n.r	-	+
Olfactory tubercle	Tu	n.r.	-	-	n.r	-	+
Extended amygdala							
Anterior amygdala	AA	n.r.	-	-	n.r.	+	+
Bed nucleus of stria terminalis medioanterior	BSTMA	-	-	-	++	+++	+++
Bed nucleus of stria terminalis medioposterior	BSTMP	-	-	-	++	+++	+++
Bed nucleus of stria terminalis laterodorsal (oval)	BSTLD	-	-	-	++	+	+
Bed nucleus of stria terminalis lateroventral	BSTLV	-	-	-	++	+++	+++
Bed nucleus of stria terminalis lateroposterior	BSTLP	-	-	-	++	+++	+++
Basolateral amygdala	BLA	-	-	-	+	+	+
Basomedial amygdala	BMA	-	-	-	+	+	+
Bed nucleus of stria terminalis intra-amygdala division	BSTIA	n.r	-	-	n.r	++	++
Central amygdaloid nucleus, lateral	CeL	-	-	-	+	+	+
Central amygdaloid nucleus, capsular	CeC	-	-	-	n.r.	++	++
Central amygdaloid nucleus, medial	CeM	-	-	-	+	++	++
Cortico-amygdala	CoA	n.r.	-	-	n.r.	+	+
Medial amygdaloid nucleus, posterodorsal	MePD	n.r.	-	+	n.r.	++	++
Medial amygdaloid nucleus, posteroventral	MePV	n.r.	-	-	n.r.	++	++
N. lat. olfactory tract	NLOT	n.r.	-	-	n.r.	+	+
Stria terminalis	st	n.r	-	-	n.r.	+	+
Basal ganglia							
Accumbens n., core	AcbC	-	-	-	+	++	++
Accumbens n., shell	AcbSh	-	-	-	n.r.	++	+++
Caudate putamen	CPu	+/-	-	-	+	+	+
Globus pallidus	GP	n.r	-	-	n.r.	+	+
Internal capsule	ic	n.r	-	-	n.r.	+	+
External capsule	ec	n.r.	-	-	n.r.	-	+
Substantia innominata	SI	n.r	-	-	n.r.	+	+

Ventral pallidum	VP	-	-	-	+	++	++
Septum							
Lat. septal n. dorsal	LSD	-	-	-	++	+++	+++
Lat. septal n. int	LSI	-	-	-	+	+	+
Lat. septal n. ventral	LSV	-	-	-	++	+++	+++
Medial septal nucleus	MS	-	-	-	+	+	+++
Septo-fimbrial n.	SFi	n.r.	-	-	n.r.	+	+
Septo-hippocampal n.	SHi	n.r	-	-	n.r	+	+
N. horizontal limb of the diagonal band	HDB	-	-	-	+	+	+
N. vertical limb of the diagonal band	VDB	-	-	-	+/-	+	+
Diencephalon							
Hypothalamus							
Anteroventral periventricular n.	AVPe	n.r.	+++	+++	n.r	+++	+++
Rostral periventricular area	RP3V	n.r.	+++	+++	n.r.	+++	+++
Anterior hypothalamic area anterior	AHA	n.r	-	-	n.r.	++	++
Anterior hypothalamic area posterior	AHp	n.r	+	+	+	++	++
Arcuate nucleus	Arc	+	++	++	+++	++++	++++
Dorsal hypothalamic	DH	-	++	++	+	+	+
Dorsomedial hypothalamic area	DM	+++	++	++	++	++	++
Lat. hypothalamic area	LH	-	-	-	+	+	+
Lat. preoptic area	LPO	-	-	-	+	++	++
Medial preoptic area	MPA	-	-	-	+	++	++
Medial preoptic n.	MnPO	-	-	-	+	+++	+++
Parastrial nucleus	PS	-	-	-	+++	+++	+++
Paraventricular hypothalamic n.	PVN	+	-	-	+	+	++
Paraventricular hypothalamic n. medial magnocellular div	PVNmm	n.r	-	-	n.r.	+++	+++
Pa hypothalamic n. lateral magnocellular div.	PVNlm	n.r	-	-	n.r.	+	+
Pa hypothalamic n. lateral parvocellular div.	PVNmp	n.r	-	-	n.r.	+++	+++
Periventricular hypothalamic n. anterior	PVa	n.r	-	-	n.r.	++	++
Premammillary n. ventral	PMV	n.r	-	-	n.r.	++	+++
Posterior hypothalamic area	PH	-	-	-	+	+	+
Retrochiasmatic area	RCh	-	-	-	+	+	+
Supraoptic nucleus	SON	-	-	-	+	++	++
Tuber cinereum area	TC	-	-	-	+	+	++
Ventral tuberomammillar n.	VTM	n.r	-	-	n.r.	++	+++
Ventromedial hypothalamic nucleus	VMH	+	-	-	+	+	+
Thalamus							
Anteromedial thalamic nucleus	AM	n.r.	-	-	n.r.	++	++
Central medial thalamic nucleus	CM	-	-	-	+	+	+
Mediodorsal thalamic nucleus	IMD	-	-	-	+	+	+
Paratenial thalamic nucleus	PT	-	-	-	+	+	+
Paraventricular thalamic nucleus	PV	-	-	-	+++	++++	++++
Reuniens thalamic nucleus	Re	-	-	-	+	+	+
Rhomboid thalamic nucleus	Rh	-	-	-	+	+	+
Submedius thalamic nucleus	SubD	n.r.	-	-	n.r.	+	+
Zona incerta	ZI	-	-	-	+	+	+
Epithalamus							
Habenular nucleus	Hb	-	-	-	++	++	++
Mesencephalon							
Central nucleus of the inferior colliculus	CIC	-	-	-	+	++	++
Cuneiform nucleus, dorsal part	CnFD	n.r.	-	-	n.r.	++	++
Dorsal raphe nucleus	DR	-	-	-	+	++	++
Deep mesenceph. n.	DpMe	-	-	-	+	+	+
Interpeduncular n.	IP	n.r.	-	-	n.r.	+	+
Median raphe n.	MnR	-	-	-	+	+	+
Periaqueductal gray, lateral	LPAG	n.r.	-	-	n.r.	++	++
Periaqueductal gray dorsomedial	DMPAG	+/-	-	-	+++	+++	+++
Substantia nigra	SN	-	-	-	+	+	+

Superior colliculus, intermediate and deep gray layer	DpG	-	-	-	+	+	+
Supramammilary n.	SuM	-	-	-	+	+	+
Ventral tegmental area	VTA	n.r.	-	-	n.r.	+	+
Metencephalon and myelencephalon							
Ambiguus nucleus	Amb	-	-	-	+	+	+
Area postrema	AP	n.r.	-	-	n.r	+++	+++
Caudoventrolateral reticular nucleus	CVL	+	-	-	+	++	++
Dorsomedial tegmental area	DMTg	n.r.	-	-	n.t.	+	+
Gigantocellular reticular nucleus	Gi	-	-	-	+	++	++
Intermediate reticular nucleus	IRt	-	-	-	++	++	++
Lateral parabrachial nucleus	LPB	-	-	-	+++	++++	++++
Lateral reticular nucleus	LRt	+			++	++	++
Lateral superior olive	LSO	-	-	-	++	+	+
Locus coeruleus	LC	-	-	-	++	+++	+++
Medial vestibular nucleus, magnocellular part	MVeMC	n.r.	-	-	n.r..	++	++
Medioventral periolivary nucleus	MVPO	n.r.	-	-	n.r.	+++	+++
Medullary reticular nucleus, dorsal part	MdD	-	-	-	+	++	++
Medullary reticular nucleus, ventral part	MdV	-	-	-	+	+	+
Nucleus of the solitary tract	Sol	+++	++	++	+++	++++	++++
Parvicellular reticular nucleus	PCRt	n.r.	-	-	n.r.	++	++
Parabrachial pigmented nucleus	PBP	n.r.	-	-	n.r.	+	+
Pontine nuclei	Pn	-	-	-	+	-	-
Pontine n, brachium pontis	bpPn	n.r.	-	-	n.r.	+	+
Pontine raphe nucleus	PnR	-	-	-	+	-	-
Pontine reticular nucleus, caudal part	PnC	-	-	-	+	+	+
Pontine reticular nucleus, oral part	PnO	-	-	-	+	+	+
Principal sensorial 5 n. dorsomedial	Pr5DM	n.r.	-	-	n.r.	++++	++++
Raphe magnus nucleus	RMg	-	-	-	+	+	+
Raphe obscurus nucleus	Rob	-	-	-	+	+	+
Raphe pallidus nucleus	RPa	-	-	-	+	+	+
Rostroventrolateral reticular nucleus	RVL	-	-	-	++	+	++
Rubrospinal tract	rs	-	-	-	++	++	++
Spinal trigeminal tract	Sp5	+	-	-	+++	-	-
Spinal 3, gelatinous layer	Ge5	n.r.	-	-	n.r.	+	++++
Superior cerebellar peduncle	scp	n.r.	-	-	n.r.	+++	+++

Table caption: Distribution of kisspeptin immunoreactive (antibody GQ2) fiber distribution in mouse & rat brain with comparison of metastatin, MT from Brailoiu et al, JCN, 2005(Brailoiu, Dun et al. 2005). Semiquantitative annotations are used here: "-", not detectable; "+", weak; "++", low; "+++", moderate; "++++", intense; "+++++", very intense. Anatomical regions are ordered based on Brailoiu et al, JCN, 2005 modified based on Allen Institute Mouse Reference Atlas. **n.r**: not reported (blue color text refers to Brailoiu et al, JCN, 2005, metastatin, MT, immunohistochemistry) cell group and expression strength analysis.

It is important noting that among 116 brain regions observed with Kp fiber and terminal presence, 81 are identified as extra-hypothalamic regions that are closely involved in central sensorial processing and behavioral state control that include ventral striatal, amygdaloid nuclei and bed nucleus of stria terminalis; diencephalic habenular complex; mesencephalic superior and inferior colliculi, periaqueductal grey; metencephalic parabrachial nucleus and locus coeruleus; myelencephalic *nucleus tractus solitarii* (NTS or Sol), reticular formation and the gelatinous layer of spinal sensorial trigeminal nucleus, all closely involved in central sensorial processing and behavioral state control (*vide infra*). The distribution of kisspeptin fibers in several regions involving numerous cruc ial central sensory relays and behavioural-state control structures suggests wider participation of this peptide in other other functions besides its known participation in reproduction and energy balance. In the following sections, we describe these regions in detail.

A

A_1: Medial septum (MS)
A_2: Septo-Hippocampal Nu. (SHi)
A_3: Diagonal Band nucleus (NDB)
A_4: Ventral tuberomammillary nucleus (VTu)
A_5: Supramammillary nucleus (SuM)
A_6: Paraventricular thalamic nucleus (PVT)
A_7: Medial (MHb) and lateral (LHb) habenula
A_8: Dorsomedial eriaqueductal gray (DMPAG)
A_9: Dorsal raphe dorsal (DRD)
A_{10}: Area postrema (AP)

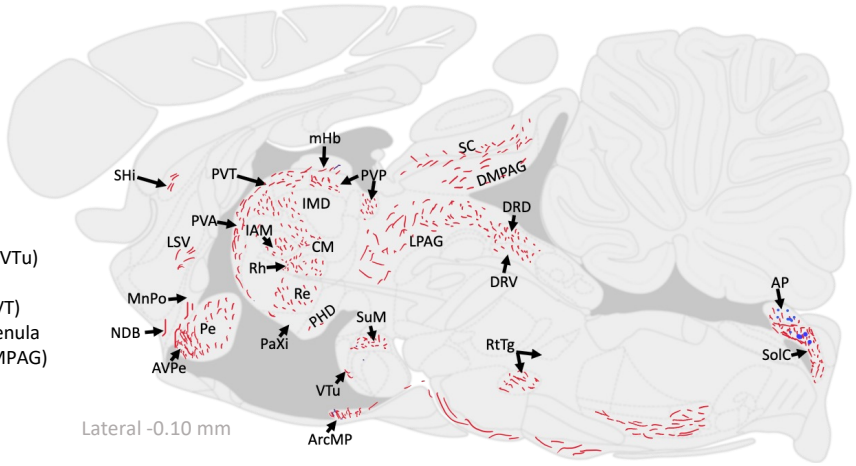

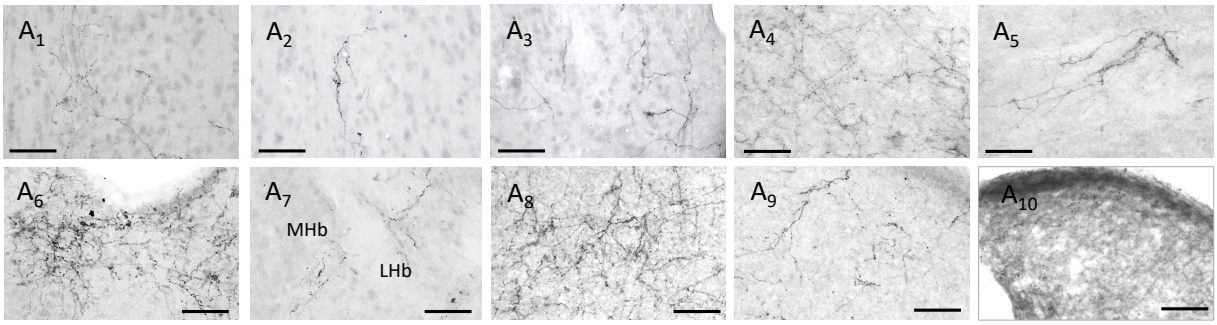

B

B_1: Lateral septum dorsal (LSD)
B_2: Septo-fimbria nucleus (SFi)
B_3: Cingulate cortex (Cg)
B_4: Anterior ventral olfactory nucleus (AOV)
B_5: Supramammillary nucleus (SuM)
B_6: Rostral periventricular area of the third ventricle (AVPe)
B_7: Arcuate nucleus (Arc)
B_8: Dorsal hypothalamus/tuber cinereum (DH/TC)
B_9: Medial preoptic nucleus (MPO)
B_{10}: Zona incerta (ZI)

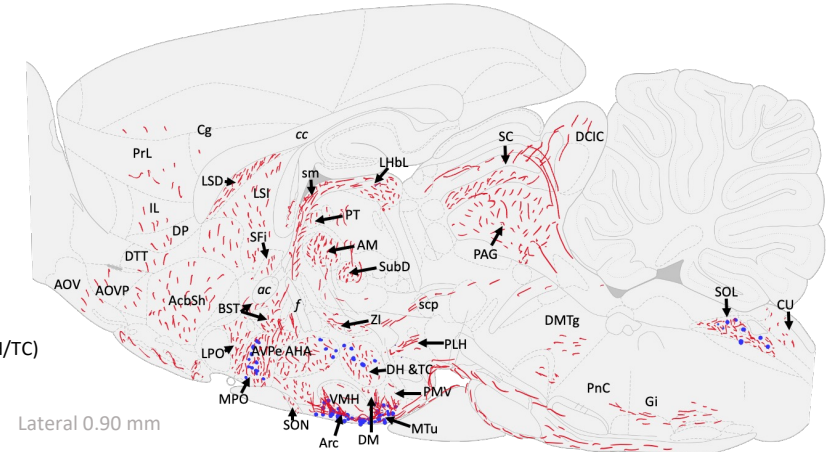

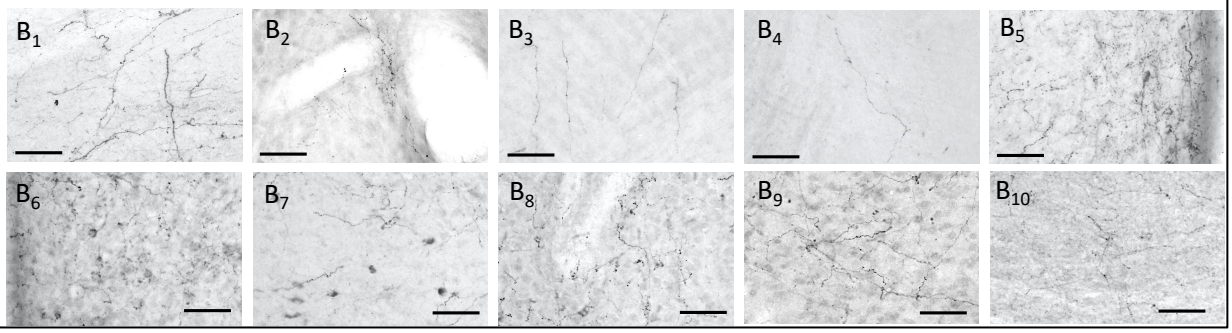

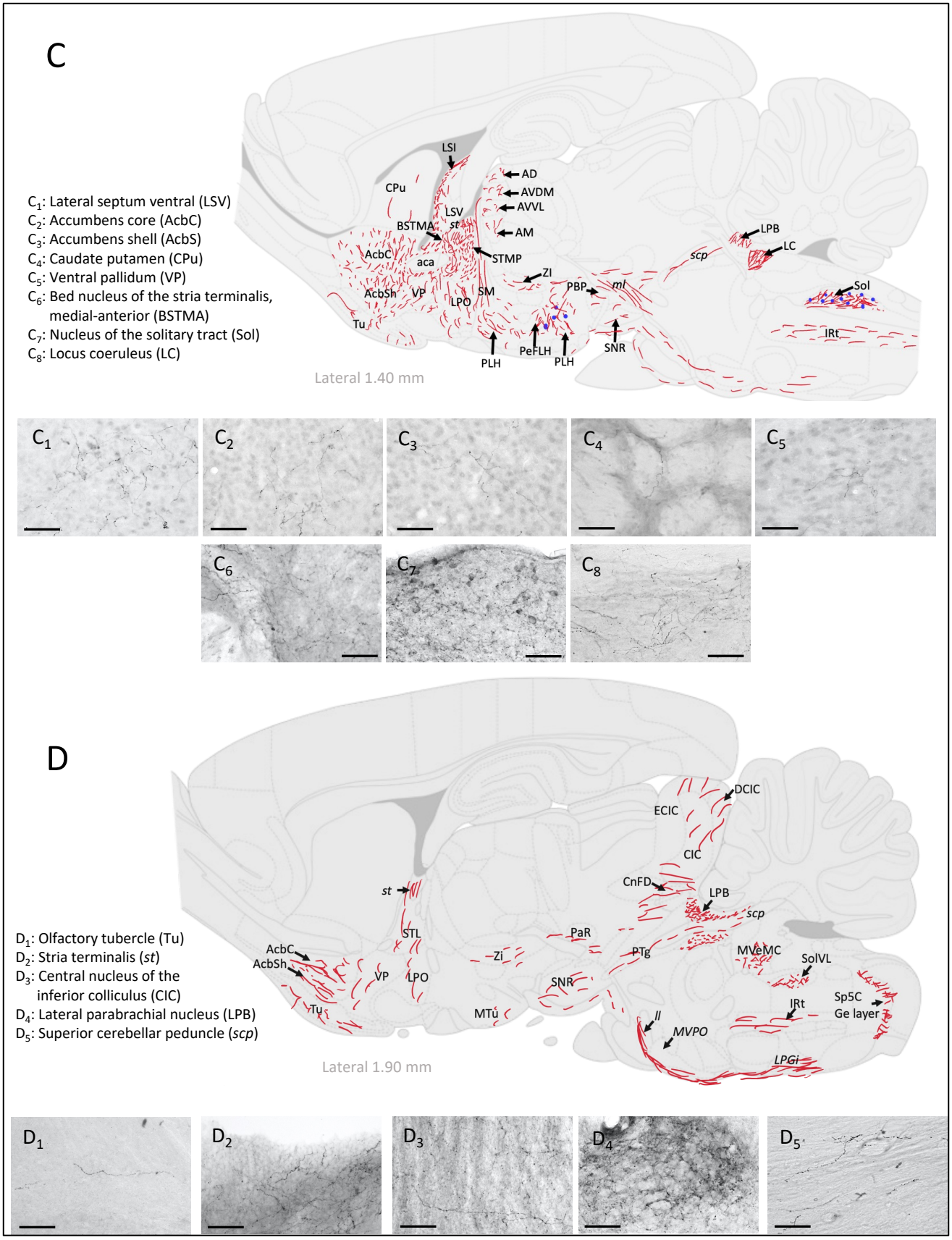
C
C1: Lateral septum ventral (LSV)
C2: Accumbens core (AcbC)
C3: Accumbens shell (AcbS)
C4: Caudate putamen (CPu)
C5: Ventral pallidum (VP)
C6: Bed nucleus of the stria terminalis, medial-anterior (BSTMA)
C7: Nucleus of the solitary tract (Sol)
C8: Locus coeruleus (LC)
LSI
CPu
AD
AVDM
AVVL
LSV
st
BSTMA
AM
AcbC
aca
STMP
ZI
AcbSh
VP
LPO
SM
PBP
ml
Tu
PLH
PeFLH
PLH
SNR
LPB
LC
scp
Sol
IRt
Lateral 1.40 mm
C1
C2
C3
C4
C5
C6
C7
C8
D
D1: Olfactory tubercle (Tu)
D2: Stria terminalis (st)
D3: Central nucleus of the inferior colliculus (CIC)
D4: Lateral parabrachial nucleus (LPB)
D5: Superior cerebellar peduncle (scp)
DCIC
ECIC
CIC
CnFD
LPB
scp
st
STL
PaR
AcbC
AcbSh
Zi
PTg
MVeMC
SolVL
VP
LPO
SNR
Tu
MTu
IRt
Sp5C
Ge layer
ll
MVPO
LPGi
Lateral 1.90 mm
D1
D2
D3
D4
D5

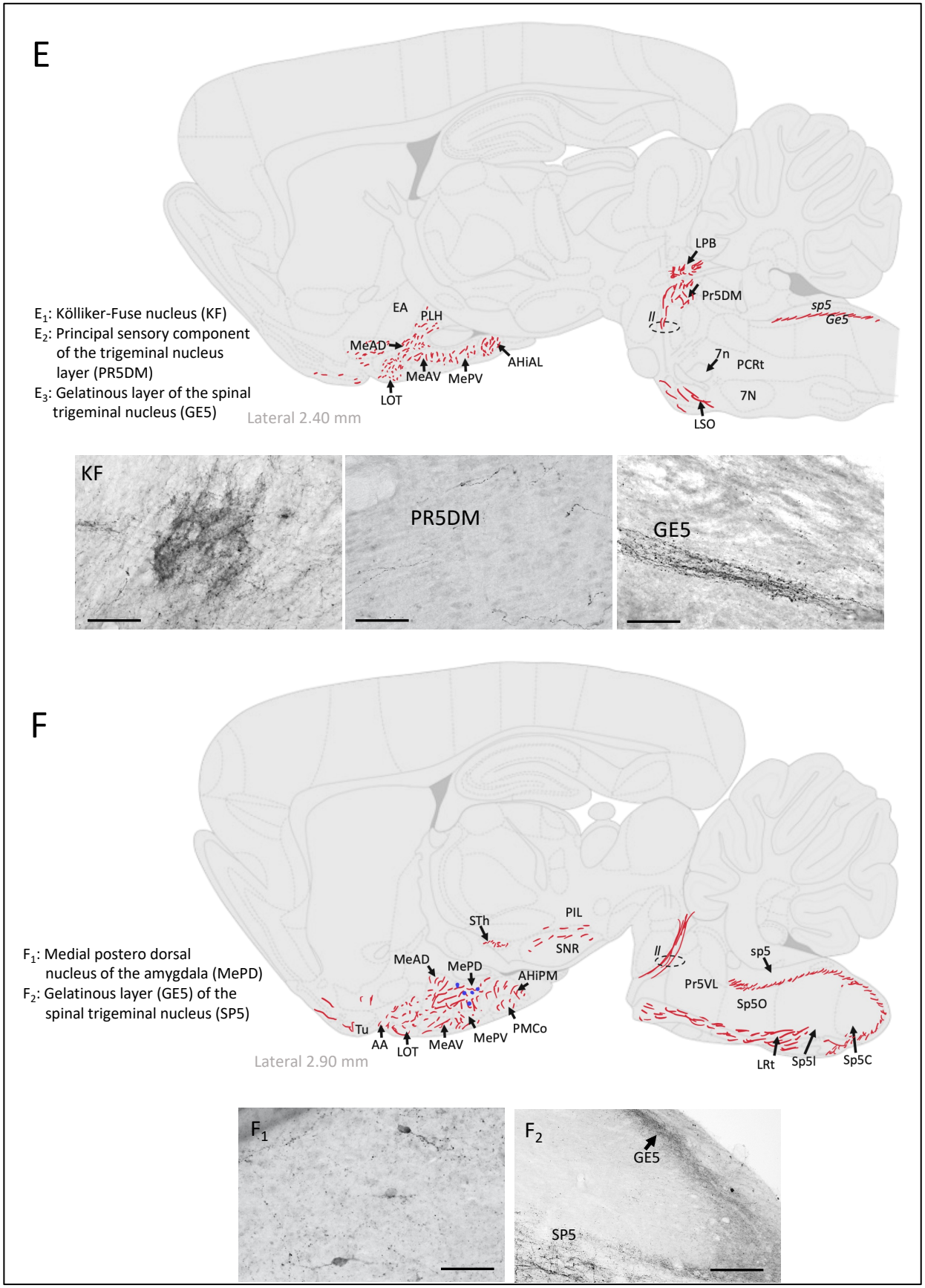
E
E1: Kölliker-Fuse nucleus (KF)
E2: Principal sensory component of the trigeminal nucleus layer (PR5DM)
E3: Gelatinous layer of the spinal trigeminal nucleus (GE5)
EA
PLH
MeAD
MeAV
MePV
AHiAL
LOT
Lateral 2.40 mm
LPB
Pr5DM
II
sp5
Ge5
7n
PCRt
7N
LSO
KF
PR5DM
GE5
F
F1: Medial postero dorsal nucleus of the amygdala (MePD)
F2: Gelatinous layer (GE5) of the spinal trigeminal nucleus (SP5)
STh
PIL
SNR
MeAD
MePD
AHiPM
Tu
AA
LOT
MeAV
MePV
PMCo
Lateral 2.90 mm
II
sp5
Pr5VL
Sp5O
LRt
Sp5I
Sp5C
F1
F2
GE5
SP5

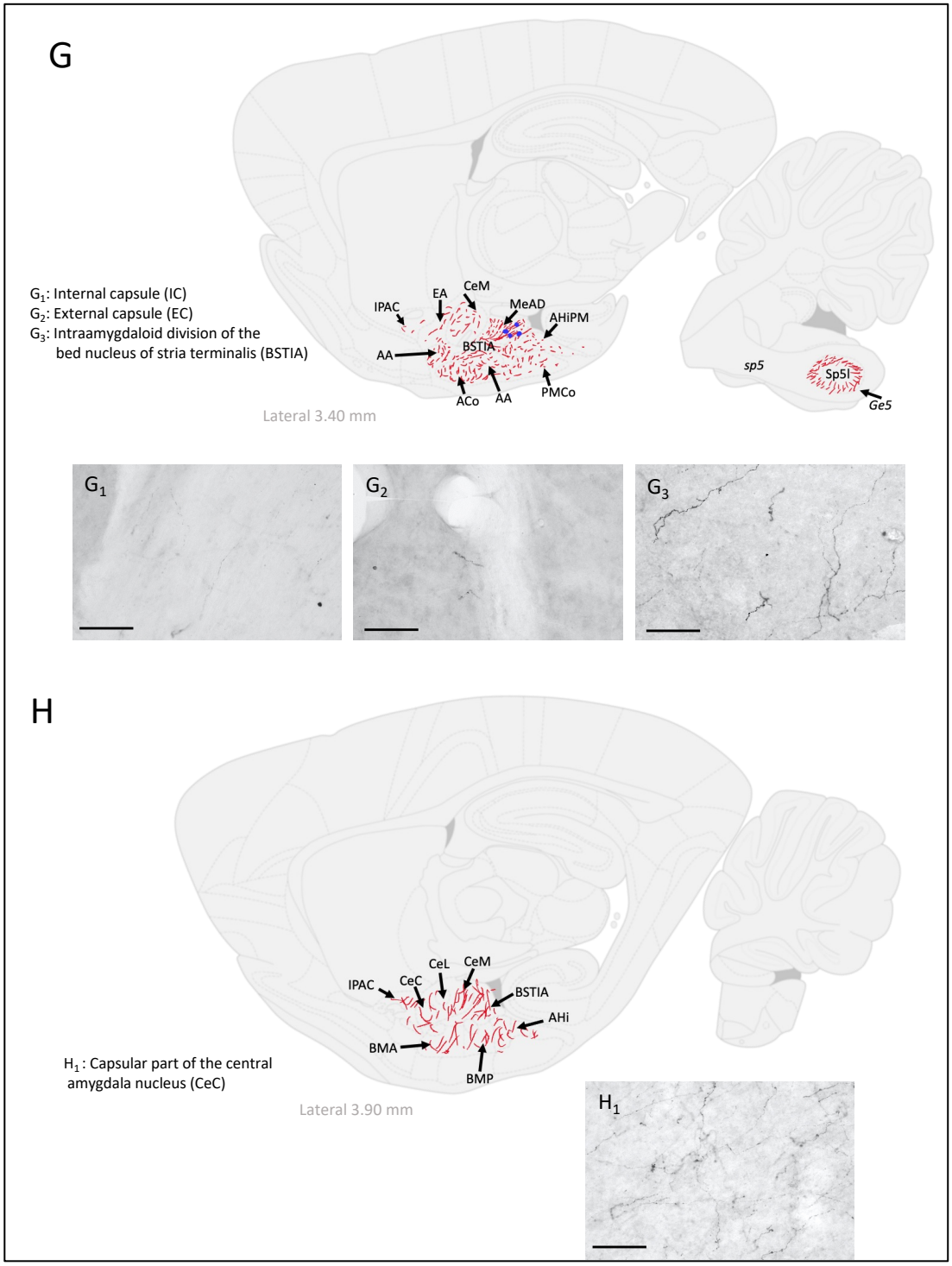

Fig. 5 Mapping of KP immunoreactive fibers and cell bodies in rat brain in ten septo-temporal planes based on microscopic observations. Blue dots represent KP-ir cell bodies and red lines represent KP-ir fibers. Relevant anatomical regions have supporting photomicrographs form IHC-DAB reactions using the GQ2 anti-kisspeptin antibody. Abbreviations: see the table 1.

3.2.1 Telencephalon

In rodent telencephalon, the most prominent Kp expression regions are located in the *lateral septal region* in male and female mice and rats. The strongest expression was observed in the dorsal lateral septal nucleus (LSD) (Fig. 5, B & B1*),* followed by ventral LS (LSV) (Fig. 5, C & C1). LS is involved in the integration of sensory and emotional information, and can modulate the activity of other brain regions involved in the regulation of behavioral states, such as the amygdala and hippocampus (Risold and Swanson 1997). Recent studies have reported the main afferents of the above regions are the subdivisions of the hippocampal formation and the main efferent regions of the LSD are the ventral tegmental area and the supramammillary nucleus, whereas the LSV project mainly to the medial hypothalamic area and medial preoptic area (Rizzi-Wise and Wang 2021). Activity of lateral septum can lead to changes in behavioral state, including increased exploratory behavioral, social interactions and decreased anxiety, particularly in response to social and emotional stimuli. These changes were reported from clinical studies with KP infusion in human subjects (Comninos, Wall et al. 2017). LS is also a key player for arousal and wakefullness, as well as for regulating processes related to mood and motivation through its extensive connections with numerous regions known to regulate affect, such as the hippocampus, amygdala, and hypothalamus. Through its connections with the mesocorticolimbic dopamine system, the LS regulates motivation, both by stimulating the activity of midbrain dopamine neurons and regulating the consequences of this activity on the ventral striatum (Sheehan, Chambers et al. 2004).

The *medial septum* (MS) also observed with mild and sparse innervation in rats and mice (Fig. 5, A & A1). This structure is crucially involved in regulating the hippocampal oscillations (Unal, Crump et al. 2018, Salib, Joshi et al. 2019) influencing a variety of behaviours, including spatial navigation, attention, learning and memory and emotional processing.

Sparse fibers in *septofimbrial nucleus* (Fig. 5, B & B2) which contains important source of cholinergic inputs to the hippocampus and the entorhinal cortex, influencing hippocampal plasticity and learning and memory under emotional stimuli; and septohippocampal (SHi, Fig. 5, A & A2) nuclei than provide important GABAergic inputs to hippocampus playing a role in the generation of hippocampal theta oscillation (Joshi, Salib et al. 2017). The above two regions are described for the first time in this study.

Similar to Brailoiu et. al (Brailoiu, Dun et al. 2005), we found sparse fibers in the *horizontal and vertical limbs of the nucleus of diagonal band of Broca* (NDB) (Fig. 5, A & A3). The diagonal band of Broca interconnects the amygdala and the septal area as well as to project particularly to hippocampus CA2 subfield which is particularly involved in memory retrieval and social functions (Dudek, Alexander et al. 2016, Liu, Lim et al. 2018). It contains the second largest cholinergic neuronal population in the brain (after the nucleus basalis of Meynert)(Semba and Fibiger 1989). It is particularly important in the aging of the brain, since the cholinergic neuronal loss in dementias has been commonly observed in human. The influence of Kp to brain cholinergic system is underinvestigated.

An interesting finding of this study was the remarkable presence of kisspeptin fibers in the *nucleus accumbens,* in both core and shell divisions (AcbC and AcbSh), with a mild density in mice and a moderate density in rats (Table 1, Fig. 5, C, C2 & C3). AcbC receives inputs from the prefrontal cortex, the amygdala, and the ventral tegmental area (VTA), which is a key component of the brain's reward system. The AcbC integrates these inputs to evaluate the salience and value of rewards and helps to regulate motivated behavior accordingly. The nucleus accumbens shell is an important brain region involved in the processing of reward-related information and the regulation of motivated behavior, including food intake, drug seeking, and social behavior (Floresco 2015).

Sparse fibers were observed in the *caudate putamen* (CPu Fig. 5, C & C4), ventral pallidus (VP, Fig. 5, C & C5), the *sustantia innominata* (SI), as well as main fibre pathways such as *the internal capsule* (ic) and *external capsule* (ec) (Fig. 5 G, G1 & G2).

In telencephalic *neocortical regions*, we found sparse fibers distributed through the *dorsal tenia tecta* (DTT) and the *dorsal peduncular* (DP), *prelimbic* (PrL) , *infralimbic* (IL), and *cingular* (Cg) cortices, regions that have not been reported in the Brailou study. The observed fibers were mainly located in layers 2/3, and no differences between species were observed (Table 1 and Fig. 5, B & B3). The *prelimbic* (PrL), *infralimbic* (IL) and *cingulate cortices* (CC) have been classically considered to be involved in mediating the role of context in the expression of fear or reward induced behaviors (Riaz, Puveendrakumaran et al. 2019) (Capuzzo and Floresco 2020, de Lima, Baldo et al. 2022). The DTT and the DP have been classically involved in olfactory information processing, and recently these two structures have been shown to send inputs with information related to psychosocial stress to the dorsomedial hypothalamus, where a cardiovascular and thermogenic sympathetic stress response can be integrated (Kataoka, Shima et al. 2020). In other areas classically related to the processing of olfactory information, such as the *ventral and ventroposterior* of the *anterior olfactory nucleus*, (AOV and AOVP) and the *olfactory tubercle* (Tu), we found sparse fibers only in the rat (Tab. 1, Fig. 5, B, B4, D & D1).

In the *amygdalar complex*, we confirm the Kp-ir+ cell population is mainly confined within the *medial amygdala's postero-dorsal division* (MePD) which has been reported already elsewhere (Gresham, Li et al. 2016, Pineda, Plaisier et al. 2017) (Tab. 2 & Fig. 5, F & F1). Kisspeptin immunolabelled neuron in the MePD and an axon terminal process were observed to innervated the adjacent nucleus of the stria terminalis intraamygdaloid division and the stria terminalis.

In relation to density of fibers in the amygdalar complex, regions with a moderate/intense density of fibers were found within the septal part of the *bed nucleus of the stria terminalis* (BSTMA, BSTMP, BSTLV and BSTLP, Fig. 5, C & C6). The *temporal intra-amygdala division of the BST* (BSTIA, Fig. 5, G & G3) showed a selective expression of Kp fibers. Other regions in the extended amygdala that also showed mild expression of Kp fibers were the central amygdalar nucleus (CeC and CeM Fig. 5, H & H1) and the medial amygdalar nucleus (MePD and MePV Fig. 5, F & F1). Sparse fibers were found in the *oval nucleus of the stria terminalis* (BSTLD), the *basolateral amygdala* (BLA), the *basomedial amygdala* (BMA), the *lateral parte of the central amygdalar nucleus* (CeL), the *cortico-amygdala* (CoA) the *nucleus of the lateral olfactory tract* (NLOT) and the *stria terminalis* (*st*, Fig. 5, D & D2). Compared with the study of Brailou et al, here we report the presence of fibers in the anterior, medial, and cortical amygdala and the intra-amygdaloid division of the stria terminalis (Tab. 2).

3.2.2. Diencephalon

We have described the chemoanatomical features at mRNA level in the figures 1- 4. Here the evidence at peptide expression level are described. The *hypothalamus* is the region where three of the five Kp neuronal populations have been reported, i.e. the rostromedial population mainly located in the *medial preoptic area* (MPO, Fig. 1, Fig. 5, B & B9) and in the *anteroventral periventricular area* (AVPe, Fig. 1, Fig. 5, B & B6). After a careful analysis of immunoreacted serial sections, following the pathways of the labelled fibers, we identified some extrahypothalamic regions targets of these MPO/AVPe GABA/kisspeptin/dynorphin neurons. Ascending fibers travel lateral-dorsal-caudally toward the *stria medularis* (*sm*), and the *stria terminalis* (*st*) conduction systems (Fig. 5, D & D2). In their path, they extensively innervate the *bed nucleus of the stria terminalis* (Tab. 2). Kisspeptin fibers mainly located in the border between the *medial (MHb) and lateral (LHb) habenula* (Fig. 5, A & A7), it is worth noting that the main input to the habenula is the stria medularis (*sm*). Other fibers originating in the MPO/AVPV region travel to innervate the *organum vasculosum of the lamina terminalis* (OVLT) and then ascend dorsally and laterally to innervate the *accumbens core* (AcbC) and the *lateral septum* regions.

The caudal periventricular area and ventral periventricular areas of the *arcuate nucleus* (Arc, Fig. 2, Fig. 5, B & B7) and the population of weakly Kp immunopositive cells scattered in the *medio-lateral dorsal hypothalamic area* (DH) spanning from the posterior part of the *anterior hypothalamus* (AHp) to the posterior hypothalamus (PH), centred in the *tuber-cinerum area* (TC) (Fig. 5, B & B8). All the above regions have high-moderate densities of Kp-ir fibers (see Tab. 2). Some targets of this neural population in the *posterior hypothalamus*

were identified by following the labelled axon in serially collected sections in coronal and parasagittal planes. The DM/DMH neurons were observed to project to immediately located *zona incerta* (ZI), continuing posteriorly through the *superior cerebral peduncle* (*scp*) to reach the *parabrachial nucleus* (PB) and the *locus coeruleus* (LC). Some fibers originating in the Arc travelled in the base of the brain reaching the *internal capsule* (*ic*) and *optic tract* through which they travel in a path to the *subthalamic nucleus* (STh), the lateral part of the *supramammillary nucleus* (SuML) and continuing to the *central nucleus of the amygdala* (CeA).

Other relevant regions in the hypothalamus with KP fibers presence are the *medial preoptic nucleus* (MPO, Fig. 5, B & B9, together with the AVPe cells Fig. 5, B & B6), the *parastriatal nucleus* (PS), the *paraventricular nucleus medial magnocellular division* (PVNmm) and the *parvocellular division* (PVNmp), and in rat also in the ventral *premammillary nucleus* (PMV) and *ventral tuberomammillary nucleus* (VTu Fig. 5, A &A4) and *suprammamilary nucleus* (SuM Fig. 5, A, A5, B & B5). A mild density of fibers was observed in *dorsomedial hypothalamic nucleus*, MPO (Fig. 5, B & B9), lateral preoptic area, the *periventricular hypothalamic nucleus anterior* (PVa), the *supraoptic nucleus* (SO). Sparse fibers were found in the *dorsal hypothalamus* (DH, Fig. 5, B & B8), *zona incerta* (ZI, Fig. 5, B & B10), *lateral hypothalamic area* (LH), *posterior hypothalamic area* (PH), *retrochiasmatic area* (RCh), and *ventromedial hypothalamic nucleus* (VMH). The Kp system in the hypothalamus has been extensively discussed in the literature (Lehman, Hileman et al. 2013).

In the *thalamus*, the highest density of fibers was observed in the *paraventricular thalamic nucleus* (PVT, Fig. 5, A & A6) in rats and mice. Mild fibers densities were also observed in other nuclei of the thalamus, such as in the *centromedial* (CM), *mediodorsal* (MD), *paratenial* (PT), *reuniens* (Re), and *rhomboid* (Rh). The epithalamic *habenular nucleus* (Hb) showed a moderate density of fibers mainly located in the border between its medial and lateral subdivisions (Fig. 5, A & A7).

3.2.3. Mesencephalon

Within the mesencephalon, Brailoiu et al (Brailoiu, Dun et al. 2005) reported a sparse number of kisspeptin-immunoreactive fibers only in the *dorsomedial periaqueductal gray substance* (DMPAG). In our study that region had the highest density of kisspeptin fibers within the mesencephalon (Fig. 5, A & A8). However, we also visualised a mild number of fibers in the *central nucleus of the inferior colliculus* (CIC, Fig. 5, D & D3), *dorsal raphe nucleus* (DR, Fig. 5, A & A9), and sparse fibers in the *deep mesencephalic nucleus* (DpMe), *interpeduncular nucleus* (IP), *median raphe nucleus* (MnR), *substantia nigra* (SN), *intermediate and deep gray layer of the superior colliculus* (DpG), *supramammillary nucleus* (Sum), *substantia nigra pars reticulata* (SNpr) and *ventral tegmental area* (VTA). The funtional implications for those Kp projections are unknown.

3.2.4. Metencephalon and myelencephalon

In the metencephalon and myelencephalon, we observed kisspeptin immunopositive somas in the *nucleus tractus solitarius* (NTS or Sol, Fig. 4, Fig. 5, C, & C7), and *area postrema* (AP, Fig. 4, Fig. 5, A, & A10, which has been overlooked in the literature). We did not observed immunopositive neurons in the caudoventrolateral or the lateral reticular nuclei (CVL and LRt), nor the spinal trigeminal tract, as reported in Brailoiu et al (Brailoiu, Dun et al. 2005). With respect to the density of the fibers, intense (++++) labelling was found in the *lateral parabrachial nucleus* (LPB, Fig. 5, D & D4), the *Kolliker-Fuse nucleus* (KF Fig. 5, E & E1), *NTS*, (Fig. 5, C, & C7) in the dorsomedial part of the *principal sensorial component of the trigeminal nucleus* (Pr5DM, Fig. 5, E, E2). The rat brain also showed intense Kp labeling in the *gelatinous layer and the spinal nerve 5* (Ge5, Fig. 5, E, E3, F, & F2). Moderate (+++) density was observed in the *superior cerebral peduncle* (*scp*, Fig. 5, D & D5) and *locus coeruleus* (Fig. 5, C & C8). Mild (++) intensity was observed in several nuclei of the *reticular formation*, including the *caudoventral reticular nucleus* (CVL); the *gigantocellular reticular nucleus* (Gi); the *intermediate reticular nucleus;* the *lateral reticular nucleus* (LRt); the *medullary dorsal reticular nucleus* (MdD); the *parvicellular reticular*

nucleus (PCRt) and the *rostroventrolateral reticular nucleus* (RVL). Sparse (+) fibre density was observed in the *ambiguus nucleus* (Amb); *lateral superior olive* (LSO); *ventral medullary reticular nucleus* (MdV); in subregions of the *pontine nucleus* such as the *brachium pontis* (bpPn) *the reticular oral part* (PnO) and the *reticular caudal* part (PnC); in *the raphe magnus* (RMg), *obscurus* (Rob), *pallidus* (RPa).

3.3 Gonadal steroid sensitivity of the kisspeptin-expressing systems

Numerous reports have consolidated the idea that a network of kisspeptin neurons mainly in the MPO/AVPV and the ARH, are key regulators of the hypothalamo-pituitary-gonadal axis and that have exquisite sensitivity to feedback from gonadal hormones, with the neurons of ARH being inhibited and those in the rostral hypothalamus being potentiated by gonadal steroids (Rance 2009, Dubois, Acosta-Martinez et al. 2015, Starrett and Moenter 2023). We analysed the brains of male and female mice that underwent gonadectomy one year before perfusion, we examined the regions with the highest density of kisspeptin fibers, and assessed if the castration could modify the density of fibers. Since no difference in the direction of changes was observed between males an females, we pooled the data reported in Table 3.

In the hypothalamic arcuate nucleus (ARH), there was a clear increase in the density of cells after gonadectomy. Other nuclei hosting neuronal somas, such as the nucleus of tractus solitarii (Sol), the dorsal hypothalamic nucleus (DH) and dorsomedial hypothalamic area (DMH), were unaffected by gonadectomy, and the anteroventral periventricular (AVPV) and medial preoptic area (MPO) showed diminished numbers of neurons after gonadectomy.

We found no changes in the fiber density within the cerebral cortex, olfactory areas, basal ganglia, thalamus, metencephalon and myelencephalon. In extended amygdala and septal regions, gonadectomy reduced the density of fibers in all regions analyzed. In the hypothalamus, the fiber density of some nuclei showed reductions (AVPV, MPO, AH, LPO, MPA, and PS), while other nuclei showed no change (DH, DMH, ZI, LH, PVN, PH, RCh, SO, TC, VMH). In the mesencephalon, there was a reduction of fibers in the periaqueductal grey (PAG), substantia nigra (SN), superior colliculus (SpC) and supramammillary nucleus (SuM).

Table 3. Gonadal sensitivity of kisspeptin expressing networks

Structure	Abbr	Cells GNX vs. Control (G vs C)	Fibers desnsity GNX vs. Control (G vs C)
Telencephalon			
Cerebral cortex (ctx)			
Cingular ctx	Cg1	n.a	G ≈ C
Prelimbic ctx	PrL	n.a	G ≈ C
Infralimbic ctx	IL	n.a	G ≈ C
Dorsal peduncular ctx	DP	n.a	G ≈ C
Dorsal tenia tecta	DTT	n.a	G ≈ C
Ventral orbital ctx	VO	n.a	G ≈ C
Olfactory area (n: nucleus)			
Anterior olfactory n.	AON	n.a	G ≈ C
Olfactory tubercle	Tu	n.a	G ≈ C
Extended amygdala			
Bed n stria terminalis medioanterior	BSTMA	n.a	G < C
Bed n stria terminalis mediopoterior	BSTMP	n.a	G < C
Bed n stria terminalis laterodorsal	BSTLD	n.a	G < C
Bed n stria terminalis lateroventral	BSTLV	n.a	G < C
Bed n stria terminalis lateroposterior	BSTLP	n.a	G < C
Basolateral amygdala	BLA	n.a	G < C
Basomedial amygdala	BMA	n.a	G < C
Bed n. stria terminalis intra-amygdala div	BSTIA	n.a	G < C
Central amygdaloid nucleus, lateral	CeL	n.a	G < C
Central amygdaloid nucleus, capsular	CeC	n.a.	G < C
Central amygdaloid nucleus, medial	CeM	n.a	G < C
Medial amygdaloid nucleus, posterodorsal	MePD	n.a.	G < C
Medial amygdaloid nucleus, posteroventral	MePV	n.a.	G < C
Anterior amygdala	AA	n.a.	G < C
Cortico-amygdala	CoA	n.a.	G < C
N. lat. olfactory tract	NLOT	n.a.	G < C

Structure	Abbr	Cells GNX vs. Control (G vs C)	Fiber density GNX vs. Control (G vs C)
Basal ganglia			
Accumbens n., core	AcbC	n.a	G ≈ C
Accumbens n., shell	AcbSh	n.a	G ≈ C
Caudate putamen	CPu	n.a	G ≈ C
Substantia innominata	SI	n.a	G ≈ C
Septum			
Lat. septal n. dorsal	LSD	n.a	G < C
Lat. septal n. int	LSI	n.a	G < C
Lat. septal n. ventral	LSV	n.a	G < C
Medial septal nucleus	MS	n.a	G < C
Septohippocampal n.	SHi	n.a	G < C
N. horizontal limb of the diagonal band	HDB	n.a	G ≈ C
N. vertical limb of the diagonal band	VDB	n.a	
Diencephalon			
Hypothalamus			
Anteroventral periventricular n.	AVPe	G < C	G < C
Rostral periventricular area	RP3V	G < C	G < C
Anterior hypothalamic area	AH	n.a.	G < C
Arcuate nucleus	Arc	G > C	G > C
Dorsal hypothalamic	DH	G ≈ C	G ≈ C
Dorsomedial hypothal. area	DM	G≈C	G ≈ C
Zona incerta	ZI	n.a.	G ≈ C
Lat. hypothal. area	LH	n.a.	G ≈ C
Lat. preoptic area	LPO	n.a.	G < C
Medial preoptic area	MPA	n.a.	G < C
Medial preoptic n.	MPO	n.a.	G < C
Parastrial nucleus	PS	n.a.	G < C
Paraventricular hypothalamic n.	PVN	n.a.	G ≈ C
Posterior hypothalamic area	PH	n.a.	G ≈ C
Retrochiasmatic area	RCh	n.a.	G ≈ C
Supraoptic nucleus	SO	n.a.	G ≈ C
Tuber cinereum area	TC	n.a.	G ≈ C
Ventromedial hypothalamic nucleus	VMH	n.a.	G ≈ C

Structure	Abbr	Cells GNX vs. Control (G vs C)	Fiber density GNX vs. Control (G vs C)
Metencephalon and myelencephalon			
Ambiguus nucleus	Amb	n.a.	G ≈ C
Caudoventrolateral reticular nucleus	CVL	n.a.	G ≈ C
Gigantocellular reticular nucleus	Gi	n.a.	G ≈ C
Intermediate reticular nucleus	IRt	n.a.	G ≈ C
Lateral parabrachial nucleus	LPB	n.a.	G ≈ C
superior cerebellar peduncle	scp	n.a.	G ≈ C
Lateral reticular nucleus	LRt	n.a.	G ≈ C
Lateral superior olive	LSO	n.a.	G ≈ C
Locus coeruleus	LC	n.a.	G ≈ C
Medullary reticular nucleus, dorsal part	MdD	n.a.	G ≈ C
Medullary reticular nucleus, ventral part	MdV	n.a.	G ≈ C
Nucleus of the solitary tract	Sol	G ≈ C	G ≈ C
Parvicellular reticular nucleus	PCRt	n.a.	G ≈ C
Pontine nuclei	Pn	n.a.	G ≈ C
Pontine raphe nucleus	PnR	n.a.	G ≈ C
Pontine reticular nucleus, caudal part	PnC	n.a.	G ≈ C
Pontine reticular nucleus, oral part	PnO	n.a.	G ≈ C
Raphe magnus nucleus	RMg	n.a.	G ≈ C
Raphe obscurus nucleus	Rob	n.a.	G ≈ C
Raphe pallidus nucleus	RPa	n.a.	G ≈ C
Rostroventrolateral reticular nucleus	RVL	n.a.	G ≈ C
Rubrospinal tract	rs	n.a.	G ≈ C
Spinal trigeminal tract	sp5	n.a.	G ≈ C

Structure	Abbr	Cells GNX vs. Control (G vs C)	Fiber desnity GNX vs. Control (G vs C)
Thalamus			
Central medial thalamic nucleus	CM	n.a.	G ≈ C
Habenular nucleus	Hb	n.a.	G ≈ C
Mediodorsal thalamic nucleus	MD	n.a.	G ≈ C
Paratenial thalamic nucleus	PT	n.a.	G ≈ C
Paraventricular thalamic nucleus	PV	n.a.	G ≈ C
Reuniens thalamic nucleus	Re	n.a.	G ≈ C
Rhomboid thalamic nucleus	Rh	n.a.	G ≈ C
Mesencephalon			
Central nucleus of the inferior colliculus	CIC	n.a.	G ≈ C
Dorsal raphe nucleus	DR	n.a.	G ≈ C
Deep mesenceph. n.	DpMe	n.a.	G ≈ C
Median raphe n.	MnR	n.a.	G ≈ C
Periaqueductal gray	PAG	n.a.	G < C
Substantia nigra	SN	n.a.	G < C
Superior colliculus intermediate and deep	SpC	n.a.	G <C
Supramammilary n.	SuM	n.a.	G <C

Table caption: Semiquantitative comparison of kisspeptin immunoreactive cell and fiber distribution in KP expressing regions of control vs gonadectomized mice. Since no differences in the direction of changes were observed in male vs female mice the data reflected here is derived from pooled observations form both sexes. n.a.: does not apply.

4. General discussion and conclusions

Our study uses a kisspeptin antibody that recognizes a conserved epitope in kisspeptin regardless of the processed form of kisspeptin in which it is contained. These investigations are supported by detection of mRNA using dual in situ hybridization (DISH) to confirm the chemotype of the kisspeptin cell types, and, importantly, not only the small monoamine transmitters (SMATs) with which kisspeptin is co-stored, but the potential for regulation by sex steroids (i.e. expression of androgen and estrogen receptors) which potentially underlies the coordination of sexual behaviors by kisspeptin neurons acting in concert throughout the brain to coordinate sensory input triggering altered behavioral state control altering sex-related behaviors.

We found much more extensive Kp containing axon terminals in subcortical brain modulatory structures. This distribution was compared with an early comprehensive report using Phoenix anti-metastatin antibody which we found more similar to our observation than other studies in rodents. Among 116 brain regions observed with KP fiber and terminal presence, 81 are identified as extra-hypothalamic regions, including telencephalic septal, ventral striatal, amygdaloid nuclei and bed nucleus of stria terminalis; diencephalic habenular complex; mesencephalic superior and inferior colliculi, periaqueductal grey; metencephalic parabrachial nucleus and locus coeruleus; myelencephalic *nucleus tractus solitarii* (NTS), reticular formation and the gelatinous layer of spinal sensorial trigeminal nucleus, all closely involved in central sensorial processing and behavioral state control. Kp cells with glutamatergic type are mainly located in arcuate nucleus (Arc) and scattered in the dorso-lateral hypothalamic (DLH) region from anterior to posterior hypothalamus with higher density in the tuber cinereum region (TC); Kp cells with GABAergic type are in the rostral periventricular (RP3V) and antero-ventral periventricular (AVPe) regions, the medial amygdala postero-dorsal (MePD) and the NTS.

We confirm some of previously reported but rather overlooked kisspeptinergic neuronal populations in medial amygdala, in dorsal hypothalamus spanning from posterior part of the anterior-hypothalamus (AHp) to the posterior hypothalamus (PH), and in the solitary nucleus (NTS) of the medulla oblongata. We report that glutamatergic and/or GABAergic cell types with in these populations as well as kisspeptin co-expression with other neuropeptides including neurokinin and dynorphin. Kp bath administration in *ex-vivo* brain preparations could induce stong modification of recorded neurons´ electrical exitability (Oakley, Clifton et al. 2009), hence the intense kisspeptinergic innervation in the above described regions and the peptide release should have important physiological consequences that should be investigated. Our results provide an anatomical basis for further hypothesis generation and testing of the role of KP in central sensory and behavioral state modulation, an aspect of KP function that is still to be fully developed fundamentally, and for its translational potential.

Besides the reproduction-linked behavioral functions of the Kp system extensively reported in the literature, another topic widely discussed is kisspeptin's role in energy balance control (Navarro 2020, Yang, Zhao et al. 2023). A series of studies showed that female *Kiss1r* KO mice displayed decreased metabolism and obesity despite decreased feeding (Tolson, Garcia et al. 2014, Tolson, Garcia et al. 2016, Tolson, Marooki et al. 2019) and that kisspeptin can modulate the activity of hypothalamic hunger/satiety circuits (Fu and van den Pol 2010, Nestor, Qiu et al. 2016). However, how the neuropeptide kisspeptin modulate the plasticity of the above neural circuits is unclear. A recent study showed that after exposing mice to predator odors, there is a stress-induced hyperthermia and Fos expression in the MeA, DMH, LH, and ARC regions. Chemogenetic activation of the DMH neurons is sufficient to induce thermogenesis in females (Jovanovic, Pool et al. 2023). This study did not evaluate if those Fos-activated neurons were Kp expresing neurons, however, according to our data, those neurons are likely to be Kp neurons due to its close anatomical locations in the precise regions where we report here the presence of kisspeptinergic neurons.

Regarding locomotion, some reports suggest Kp's participation in the locomotive behavior regulation. For instance, the blood levels of Kp in anorexia nervosa patients showed an inverse correlation with their level of physical activity (Hofmann, Elbelt et al. 2017), which suggests an altered behavioral state of those patients linked with abnormal Kp plasma concentration. However, in a study in mice, Kp-13 was injected intracerebroventricularly

and an increase in locomotion was observed in the open field test as well as increased core temperature (Csabafi, Jaszberenyi et al. 2013). In another study that injected Kp-8 via ICV in Wistar rats, decreased locomotion in the open field test and increased release of GABA in the nucleus accumbens were observed (Ibos, Bodnar et al. 2021). The central KP circuits modulating locomotion and body temperature are currently unknown.

We have reported in this study that high density of Kp fibers are present in areas related to pain sensory processing, such as the principal sensorial trigeminal nucleus, the gelatinous layer of the trigeminus and in the periaqueductal gray. In the literature, only few studies have investigated Kp's role in the modulating of the perception of exteroceptive or interoceptive non-reproductive functions. It has been shown that KP-10 activates calcium signaling pathways in cultured dorsal root ganglion cells, suggesting a possible participation in pain modulation (Kelestimur, Bulut et al. 2021). Other regions classically involved in sensory processing have moderate/dense innervation of Kp fibers, *i.e.,* superior colliculus for visual processing; the inferior colliculus and superior olive for audition; the parabrachial nucleus and nucleus of the solitary tract (NTS or Sol) for gustatory processing; and the olfactory tubercle, nucleus of the olfactory tract and medial amygdala for olfaction. To our knowledge, the effect of Kp on the activity of these regions and its effect on sensory integration has not been studied.

There has been significant advance in our understanding of the critical role of kisspeptin in human sexually-related behavior in clinical studies featuring kisspeptin administration in men and women (Comninos, Wall et al. 2017). However, except for some scattered reports (e.g. (Pineda, Plaisier et al. 2017)), there has been little exploration of kisspeptin projections to areas other than LH-RH neurons of the hypothalamus. This is important because, as pointed out by Liu and Herbison (Liu and Herbison 2016), the post-synaptic effects of kisspeptin leading to behavioral effects such as increased sexual responsiveness are likely to be a) via neuromodulatory rather than direct neurotransmitter mechanisms and b) via kisspeptinergic innervation of brain areas involved in both sensorial processing and behavioral state control. Thus, a better understanding of the projection of kisspeptin neurons outside of the hypothalamus, arising from both hypothalamic and extrahypothalamic kisspeptin cell bodies, is urgently required.

Authors contribution statement

Limei Zhang
Conceptualization, data curation, formal analysis, funding acquisition, investigation, methodology, project administration, resources, supervision, validation, visualization, writing – original draft, review & editing.

Vito H. Hernandez
Conceptualization, data curation, formal analysis, investigation, methodology, project administration, resources, software, supervision, validation, visualization, writing – original draft, review & editing

Mario A. Zetter
Data curation, formal analysis, investigation, methodology, validation, review & editing

Rafael Hernández-González
Investigation, methodology, validation, resources, supervision, review & editing

Oscar René Hernández-Pérez
Investigation, methodology, validation, resources, supervision, review & editing

Ignacio Camacho-Arroyo
Resources, supervision, validation, review & editing

Lee E. Eiden
Resources, funding, supervision, validation, writing – original draft, review & editing

Robert P. Millar
Conceptualization, resources, supervision, validation, review & editing

Acknowledgement

This study was supported by grants: UNAM-DGAPA-PAPIIT-IN200121 & CONACYT-CF-G-243 (LZ); NIMH-IRP, NIH, ZIAMH0002386 (LEE). LZ and VSH were supported by sabbatical fellowship from the PASPA program of the *Dirección General de Personal Académico (DGAPA)* of the *Universidad Nacional Autónoma de México (UNAM);* MAZ was supported by the POSDOC program of DGAPA-UNAM and RPM was supported by PREI program provided of the DGAPA-UNAM for a sabbatical research stay in LZ's lab in UNAM, Mexico.

References

Brailoiu, G. C., S. L. Dun, M. Ohsawa, D. Yin, J. Yang, J. K. Chang, E. Brailoiu and N. J. Dun (2005). "KiSS-1 expression and metastin-like immunoreactivity in the rat brain." J Comp Neurol **481**(3): 314-329.

Capuzzo, G. and S. B. Floresco (2020). "Prelimbic and Infralimbic Prefrontal Regulation of Active and Inhibitory Avoidance and Reward-Seeking." J Neurosci **40**(24): 4773-4787.

Clarke, H., W. S. Dhillo and C. N. Jayasena (2015). "Comprehensive Review on Kisspeptin and Its Role in Reproductive Disorders." Endocrinol Metab (Seoul) **30**(2): 124-141.

Comninos, A. N., M. B. Wall, L. Demetriou, A. J. Shah, S. A. Clarke, S. Narayanaswamy, A. Nesbitt, C. Izzi-Engbeaya, J. K. Prague, A. Abbara, R. Ratnasabapathy, V. Salem, G. M. Nijher, C. N. Jayasena, M. Tanner, P. Bassett, A. Mehta, E. A. Rabiner, C. Honigsperger, M. R. Silva, O. K. Brandtzaeg, E. Lundanes, S. R. Wilson, R. C. Brown, S. A. Thomas, S. R. Bloom and W. S. Dhillo (2017). "Kisspeptin modulates sexual and emotional brain processing in humans." J Clin Invest **127**(2): 709-719.

Csabafi, K., M. Jaszberenyi, Z. Bagosi, N. Liptak and G. Telegdy (2013). "Effects of kisspeptin-13 on the hypothalamic-pituitary-adrenal axis, thermoregulation, anxiety and locomotor activity in rats." Behav Brain Res **241**: 56-61.

de Lima, M. A. X., M. V. C. Baldo, F. A. Oliveira and N. S. Canteras (2022). "The anterior cingulate cortex and its role in controlling contextual fear memory to predatory threats." Elife **11**.

Dhillo, W. S., O. B. Chaudhri, M. Patterson, E. L. Thompson, K. G. Murphy, M. K. Badman, B. M. McGowan, V. Amber, S. Patel, M. A. Ghatei and S. R. Bloom (2005). "Kisspeptin-54 stimulates the hypothalamic-pituitary gonadal axis in human males." J Clin Endocrinol Metab **90**(12): 6609-6615.

Dubois, S. L., M. Acosta-Martinez, M. R. DeJoseph, A. Wolfe, S. Radovick, U. Boehm, J. H. Urban and J. E. Levine (2015). "Positive, but not negative feedback actions of estradiol in adult female mice require estrogen receptor alpha in kisspeptin neurons." Endocrinology **156**(3): 1111-1120.

Dudek, S. M., G. M. Alexander and S. Farris (2016). "Rediscovering area CA2: unique properties and functions." Nat Rev Neurosci **17**(2): 89-102.

Floresco, S. B. (2015). "The nucleus accumbens: an interface between cognition, emotion, and action." Annu Rev Psychol **66**: 25-52.

Fu, L. Y. and A. N. van den Pol (2010). "Kisspeptin directly excites anorexigenic proopiomelanocortin neurons but inhibits orexigenic neuropeptide Y cells by an indirect synaptic mechanism." J Neurosci **30**(30): 10205-10219.

Gresham, R., S. Li, D. A. Adekunbi, M. Hu, X. F. Li and K. T. O'Byrne (2016). "Kisspeptin in the medial amygdala and sexual behavior in male rats." Neurosci Lett **627**: 13-17.

Hatcher, K. M., L. Costanza, A. S. Kauffman and S. B. Z. Stephens (2023). "The molecular phenotype of kisspeptin neurons in the medial amygdala of female mice." Front Endocrinol (Lausanne) **14**: 1093592.

Hofmann, T., U. Elbelt, V. Haas, A. Ahnis, B. F. Klapp, M. Rose and A. Stengel (2017). "Plasma kisspeptin and ghrelin levels are independently correlated with physical activity in patients with anorexia nervosa." Appetite **108**: 141-150.

Ibos, K. E., E. Bodnar, Z. Bagosi, Z. Bozso, G. Toth, G. Szabo and K. Csabafi (2021). "Kisspeptin-8 Induces Anxiety-Like Behavior and Hypolocomotion by Activating the HPA Axis and Increasing GABA Release in the Nucleus Accumbens in Rats." Biomedicines **9**(2).
Joshi, A., M. Salib, T. J. Viney, D. Dupret and P. Somogyi (2017). "Behavior-Dependent Activity and Synaptic Organization of Septo-hippocampal GABAergic Neurons Selectively Targeting the Hippocampal CA3 Area." Neuron **96**(6): 1342-1357 e1345.
Jovanovic, P., A. H. Pool, N. Morones, Y. Wang, E. Novinbakht, N. Keshishian, K. Jang, Y. Oka and C. E. Riera (2023). "A sex-specific thermogenic neurocircuit induced by predator smell recruiting cholecystokinin neurons in the dorsomedial hypothalamus." Nat Commun **14**(1): 4937.
Kataoka, N., Y. Shima, K. Nakajima and K. Nakamura (2020). "A central master driver of psychosocial stress responses in the rat." Science **367**(6482): 1105-1112.
Kelestimur, H., F. Bulut, S. Canpolat, M. Ozcan and A. Ayar (2021). "Kisspeptin leads to calcium signaling in cultured rat dorsal root ganglion neurons." Gen Physiol Biophys **40**(2): 155-160.
Kotani, M., M. Detheux, A. Vandenbogaerde, D. Communi, J. M. Vanderwinden, E. Le Poul, S. Brezillon, R. Tyldesley, N. Suarez-Huerta, F. Vandeput, C. Blanpain, S. N. Schiffmann, G. Vassart and M. Parmentier (2001). "The metastasis suppressor gene KiSS-1 encodes kisspeptins, the natural ligands of the orphan G protein-coupled receptor GPR54." J Biol Chem **276**(37): 34631-34636.
Lee, J. H., M. E. Miele, D. J. Hicks, K. K. Phillips, J. M. Trent, B. E. Weissman and D. R. Welch (1996). "KiSS-1, a novel human malignant melanoma metastasis-suppressor gene." J Natl Cancer Inst **88**(23): 1731-1737.
Lehman, M. N., L. M. Coolen, R. A. Steiner, G. Neal-Perry, L. Wang, S. M. Moenter, A. M. Moore, R. L. Goodman, S. Hwa-Yeo, S. L. Padilla, A. S. Kauffman, J. Garcia, M. J. Kelly, J. Clarkson, S. Radovick, A. V. Babwah, S. Leon, M. Tena-Sempere, A. Comninos, S. Seminara, W. S. Dhillo, J. Levine, E. Terasawa, A. Negron and A. E. Herbison (2018). "The 3(rd) World Conference on Kisspeptin, "Kisspeptin 2017: Brain and Beyond":Unresolved questions, challenges and future directions for the field." J Neuroendocrinol: e12600.
Lehman, M. N., S. M. Hileman and R. L. Goodman (2013). "Neuroanatomy of the kisspeptin signaling system in mammals: comparative and developmental aspects." Adv Exp Med Biol **784**: 27-62.
Liu, A. K. L., E. J. Lim, I. Ahmed, R. C. Chang, R. K. B. Pearce and S. M. Gentleman (2018). "Review: Revisiting the human cholinergic nucleus of the diagonal band of Broca." Neuropathol Appl Neurobiol **44**(7): 647-662.
Liu, X. and A. E. Herbison (2016). "Kisspeptin Regulation of Neuronal Activity throughout the Central Nervous System." Endocrinol Metab (Seoul) **31**(2): 193-205.
Lopez-Ojeda, W. and R. A. Hurley (2022). "Kisspeptin in the Limbic System: New Insights Into Its Neuromodulatory Roles." J Neuropsychiatry Clin Neurosci **34**(3): 190-195.
Merighi, A. (2018). "The histology, physiology, neurochemistry and circuitry of the substantia gelatinosa Rolandi (lamina II) in mammalian spinal cord." Prog Neurobiol **169**: 91-134.
Mikkelsen, J. D. and V. Simonneaux (2009). "The neuroanatomy of the kisspeptin system in the mammalian brain." Peptides **30**(1): 26-33.
Mills, E. G., L. Yang, A. Abbara, W. S. Dhillo and A. N. Comninos (2022). "Current Perspectives on Kisspeptins Role in Behaviour." Front Endocrinol (Lausanne) **13**: 928143.

Navarro, V. M. (2020). "Metabolic regulation of kisspeptin - the link between energy balance and reproduction." Nat Rev Endocrinol **16**(8): 407-420.
Nestor, C. C., J. Qiu, S. L. Padilla, C. Zhang, M. A. Bosch, W. Fan, S. A. Aicher, R. D. Palmiter, O. K. Ronnekleiv and M. J. Kelly (2016). "Optogenetic Stimulation of Arcuate Nucleus Kiss1 Neurons Reveals a Steroid-Dependent Glutamatergic Input to POMC and AgRP Neurons in Male Mice." Mol Endocrinol **30**(6): 630-644.
Oakley, A. E., D. K. Clifton and R. A. Steiner (2009). "Kisspeptin signaling in the brain." Endocr Rev **30**(6): 713-743.
Pineda, R., F. Plaisier, R. P. Millar and M. Ludwig (2017). "Amygdala Kisspeptin Neurons: Putative Mediators of Olfactory Control of the Gonadotropic Axis." Neuroendocrinology **104**(3): 223-238.
Rance, N. E. (2009). "Menopause and the human hypothalamus: evidence for the role of kisspeptin/neurokinin B neurons in the regulation of estrogen negative feedback." Peptides **30**(1): 111-122.
Riaz, S., P. Puveendrakumaran, D. Khan, S. Yoon, L. Hamel and R. Ito (2019). "Prelimbic and infralimbic cortical inactivations attenuate contextually driven discriminative responding for reward." Sci Rep **9**(1): 3982.
Risold, P. Y. and L. W. Swanson (1997). "Connections of the rat lateral septal complex." Brain Res Brain Res Rev **24**(2-3): 115-195.
Rizzi-Wise, C. A. and D. V. Wang (2021). "Putting Together Pieces of the Lateral Septum: Multifaceted Functions and Its Neural Pathways." eNeuro **8**(6).
Salib, M., A. Joshi, L. Katona, M. Howarth, B. R. Micklem, P. Somogyi and T. J. Viney (2019). "GABAergic Medial Septal Neurons with Low-Rhythmic Firing Innervating the Dentate Gyrus and Hippocampal Area CA3." J Neurosci **39**(23): 4527-4549.
Semba, K. and H. C. Fibiger (1989). "Organization of central cholinergic systems." Prog Brain Res **79**: 37-63.
Sheehan, T. P., R. A. Chambers and D. S. Russell (2004). "Regulation of affect by the lateral septum: implications for neuropsychiatry." Brain Res Brain Res Rev **46**(1): 71-117.
Sheikh, N. K. and A. Dua (2023). Neuroanatomy, Substantia Gelatinosa. StatPearls. Treasure Island (FL) ineligible companies. Disclosure: Anterpreet Dua declares no relevant financial relationships with ineligible companies.
Sophocleous, A. and A. I. Idris (2019). Ovariectomy/Orchiectomy in Rodents. Bone Research Protocols. A. I. Idris. New York, NY, Springer New York**:** 261-267.
Starrett, J. R. and S. M. Moenter (2023). "Hypothalamic kisspeptin neurons as potential mediators of estradiol negative and positive feedback." Peptides **163**: 170963.
Stout Steele, M. and R. A. Bennett (2011). "Clinical Technique: Dorsal Ovariectomy in Rodents." Journal of Exotic Pet Medicine **20**(3): 222-226.
Tolson, K. P., C. Garcia, I. Delgado, N. Marooki and A. S. Kauffman (2016). "Metabolism and Energy Expenditure, But Not Feeding or Glucose Tolerance, Are Impaired in Young Kiss1r KO Female Mice." Endocrinology **157**(11): 4192-4199.
Tolson, K. P., C. Garcia, S. Yen, S. Simonds, A. Stefanidis, A. Lawrence, J. T. Smith and A. S. Kauffman (2014). "Impaired kisspeptin signaling decreases metabolism and promotes glucose intolerance and obesity." J Clin Invest **124**(7): 3075-3079.

Tolson, K. P., N. Marooki, A. Wolfe, J. T. Smith and A. S. Kauffman (2019). "Cre/lox generation of a novel whole-body Kiss1r KO mouse line recapitulates a hypogonadal, obese, and metabolically-impaired phenotype." Mol Cell Endocrinol **498**: 110559.
Unal, G., M. G. Crump, T. J. Viney, T. Eltes, L. Katona, T. Klausberger and P. Somogyi (2018). "Spatio-temporal specialization of GABAergic septo-hippocampal neurons for rhythmic network activity." Brain Struct Funct **223**(5): 2409-2432.
Yang, F., S. Zhao, P. Wang and W. Xiang (2023). "Hypothalamic neuroendocrine integration of reproduction and metabolism in mammals." J Endocrinol **258**(3).
Zhang, L. and V. S. Hernandez (2013). "Synaptic innervation to rat hippocampus by vasopressin-immuno-positive fibres from the hypothalamic supraoptic and paraventricular nuclei." Neuroscience **228**: 139-162.
Zhang, L., V. S. Hernandez, C. R. Gerfen, S. Z. Jiang, L. Zavala, R. A. Barrio and L. E. Eiden (2021). "Behavioral role of PACAP signaling reflects its selective distribution in glutamatergic and GABAergic neuronal subpopulations." Elife **10**.
Zhang, L., V. S. Hernandez, J. D. Swinny, A. K. Verma, T. Giesecke, A. C. Emery, K. Mutig, L. M. Garcia-Segura and L. E. Eiden (2018). "A GABAergic cell type in the lateral habenula links hypothalamic homeostatic and midbrain motivation circuits with sex steroid signaling." Transl Psychiatry **8**(1): 50.
Zhang, L., V. S. Hernandez, M. A. Zetter and L. E. Eiden (2020). "VGLUT-VGAT expression delineates functionally specialised populations of vasopressin-containing neurones including a glutamatergic perforant path-projecting cell group to the hippocampus in rat and mouse brain." J Neuroendocrinol **32**(4): e12831.

1.